CRABP-I is related to Alzheimer's disease[14] and CRABP-II is associated with neuroblastoma,[15] Wilms tumor,[15] and head and neck squamous cell carcinoma (HNSCC).[16] Therefore, CRABPs could be target proteins for treatment of these diseases. However, compounds which directly control the function(s) of CRABPs have never been reported, and the biological/physiological roles of these proteins remain unclear. Thus, small molecules that suppress the function of CRABPs would be of great interest, not only as tools for probing the biological/physiological roles of CRABPs but also as potential therapeutic agents for Alzheimer's disease and cancer.

Herein, we describe a protein knockdown approach targeting CRABPs focusing on (i) design and synthesis of hybrid molecules consisting of MeBS (**2**) and ATRA (**3**) connected via a spacer, (ii) CRABPs-degrading activity of the hybrid molecules, (iii) the mechanism through which CRABP-degradation is induced by the hybrid molecules, and (iv) inhibitory activity of the hybrid molecules on tumor invasion in cell-based assay.

Results and Discussion

Molecular Design. We speculated that the E3 ligase activity of cIAP1 might be harnessed for targeted protein degradation. In other words, if cIAP1 and a target protein could be induced to form an artificial (nonphysiological) complex, the target protein should be ubiquitinated by cIAP1, as cIAP1 ubiquitinates proteins that are bound to it. Thus, we hypothesized that hybrid small molecules, i.e., conjugates of ligands for target proteins with membrane-permeable MeBS (**2**), might induce selective degradation of the target proteins (Scheme 1c). Such hybrid small molecules were expected to strictly mimic the cognate complex for ubiquitination and to have sufficient membrane permeability for practical application.

To test this idea, we designed the hybrid molecules **4**, consisting of MeBS (**2**) coupled via a spacer moiety to ATRA (**3**), the specific ligand of CRABPs. The spacer was linked to the ester position of MeBS (**2**) and to the C4 position of ATRA (**3**). These positions were selected on the basis of our previous studies showing that (i) introduction of a bulky substituent at the ester moiety of MeBS (**2**) does not affect the binding affinity for cIAP1,[10b] (ii) introduction of a substituent at the C4 position of ATRA (**3**) does not affect the binding affinity for CRABP,[17] and (iii) the latter modification causes loss of ATRA's binding affinity for RARs (see our previous report and X-ray structure in the Supporting Information, Figure S1).[18] Observations (ii) and (iii) suggest that **4** would selectively bind to CRABPs, but not to RARs. Since the length of the spacer is likely to influence the efficiency of ubiquitination of target proteins, we designed

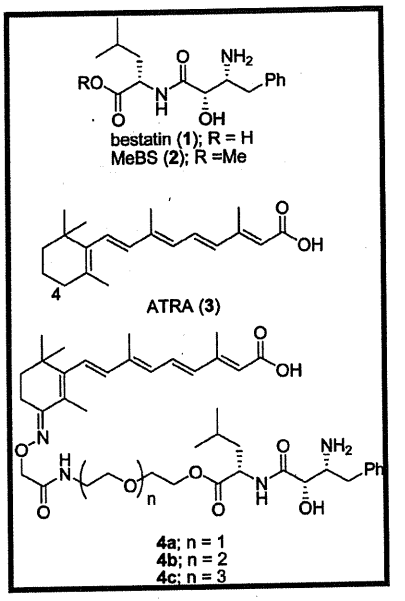

Figure 1. Structures of bestatin (**1**), MeBS (**2**), ATRA (**3**), and compounds **4**.

and synthesized three compounds **4a**–**c** (Figure 1) with different spacer lengths.

Synthesis. The designed compounds were synthesized as illustrated in Scheme 2. Compound **5** was prepared from ATRA (**3**) by esterification with 2-cyanoethyl alcohol, oxidation with excess MnO_2, and oximation with *O*-(carboxylmethyl)hydroxylamine.[18d,19] Compound **6** was prepared by protection of the amino group of bestatin (**1**). Condensation of compound **6** with alcohols **7a**–**c**[20] in the presence of 1-ethyl-3-(3-dimethylaminopropyl)carbodiimide (EDCI) and 1-hydroxybenzotriazole hydrate (HOBt·H_2O) afforded esters **8a**–**c**. Amines **9a**–**c** were obtained from compounds **8a**–**c** by removal of the Boc group under acidic conditions. Amidation of compound **5** and amines **9a**–**c** gave amides **10a**–**c** in good yield. Deprotection of the 9-fluorenylmethyloxycarbonyl (Fmoc) groups and 2-cyanoethyl groups of compounds **10a**–**c** with tetrabutylammonium fluoride (TBAF)[21] and 1,8-diazabicyclo[5.4.0]undec-7-ene (DBU)[22] gave compounds **4a**–**c**.

Decrease of CRABPs by the Synthesized Compounds. MOLT-4 cells express cIAP1 and CRABP-I (but not CRABP-II), and HT1080 cells express cIAP1 and CRABP-II (but not CRABP-I), as examined by Western blotting analysis (Supporting Information, Figure S2). Therefore, we examined the effects of **4** on the levels of CRABP-I in MOLT-4 cells and CRABP-II in HT1080 cells by Western blot analysis. As shown in Figure 2a, compounds **4** induced a dose-dependent decrease of CRABP-I protein in MOLT-4 cells. Compound **4b** seemed to be the most potent, and **4a** seemed to be the least potent among

(14) Uhrig, M.; Brechlin, P.; Jahn, O.; Knyazev, Y.; Weninger, A.; Busia, L.; Honarnejad, K.; Otto, M.; Hartmann, T. *BMC Med.* **2008**, *6*, 38–49.
(15) (a) Gupta, A.; Williams, B. R.; Hanash, S. M.; Rawwas, J. *Cancer Res.* **2006**, *66*, 8100–8108. (b) Gupta, A.; Kessler, P.; Rawwas, J.; Williams, B. R. *Exp. Cell Res.* **2008**, *314*, 3663–3668.
(16) Vo, H. P.; Crowe, D. L. *Anticancer Res.* **1998**, *18*, 217–224.
(17) Chapman, J. M.; Curley, R. W., Jr. *Protein Expr. Purif.* **1990**, *1*, 63–69.
(18) (a) Crettaz, M.; Baron, A.; Siegenthaler, G.; Hunziker, W. *Biochem. J.* **1990**, *272*, 391–397. (b) Kleywegt, G. J.; Bergfors, T.; Senn, H.; Le, M. P.; Gesell, B.; Shudo, K.; Jones, T. A. *Structure* **1994**, *2*, 1241–1258PDB ID 1CBS. (c) Renaud, J. P.; Rochel, N.; Ruff, M.; Vivat, V.; Chambon, P.; Gronemeyer, H.; Moras, D. *Nature* **1995**, *378*, 681–689PDB ID 2LBD. (d) Shimazawa, R.; Sanda, R.; Mizoguchi, H.; Hashimoto, Y.; Iwasaki, S.; Tanaka, H.; Kagechika, H.; Shudo, K. *Biochem. Biophys. Res. Commun.* **1991**, *179*, 259–265.
(19) Patel, J. B.; Huynh, C. K.; Handratta, V. D.; Gediya, L. K.; Brodie, A. M.; Goloubeva, O. G.; Clement, O. O.; Nanne, I. P.; Soprano, D. R.; Njar, V. C. *J. Med. Chem.* **2004**, *47*, 6716–6729.
(20) (a) Dekker, F. J.; de Mol, N. J.; van Ameijde, J.; Fischer, M. J. E.; Ruijtenbeek, R.; Redegeld, F. A. M.; Liskamp, R. M. J. *ChemBioChem* **2002**, *3*, 238–242. (b) Lebeau, L.; Oudet, P.; Mioskowski, C. *Helv. Chim. Acta* **1991**, *74*, 1697–1706.
(21) Kita, Y.; Maeda, H.; Takahashi, F.; Fujui, S.; Ogawa, T.; Hatayama, K. *Chem. Pharm. Bull.* **1994**, *42*, 147–50.
(22) Bernardes, G. J.; Grayson, E. J.; Thompson, S.; Chalker, J. M.; Errey, J. C.; El Oualid, F.; Claridge, T. D.; Davis, B. G. *Angew. Chem., Int. Ed.* **2008**, *47*, 2244–2247.

Scheme 2. Synthesis of Compounds **4**[a]

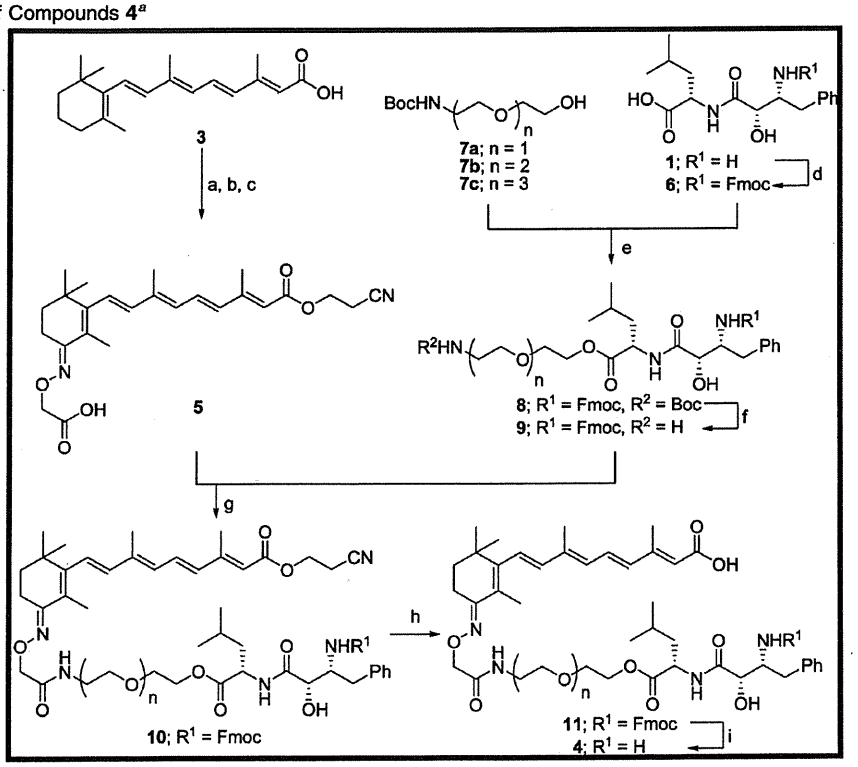

[a] Reagents and conditions: (a) 2-cyanoethyl alcohol, 1-ethyl-3-(3-dimethylaminopropyl)carbodiimide (EDCI), *N,N*-dimethylaminopyridine (DMAP), CH_2Cl_2, room temperature, 18 h, 90%; (b) MnO_2, CH_2Cl_2, room temperature, 22 h, 36%; (c) *O*-(carboxylmethyl)hydroxylamine, pyridine, room temperature, 17 h, 100%; (d) 9-fluorenylmethyloxycarbonyl chloride (FmocCl), K_2CO_3, THF, H_2O, room temperature, 24 h, 97%; (e) EDCI,1-hydroxybenzotriazole hydrate (HOBt·H_2O), *i*-Pr_2NEt, CH_2Cl_2, room temperature, 24 h, 14−51% (from **6**); (f) HCl, 1,4-dioxane, room temperature, 1 h, quant; (g) EDCI, HOBt·H_2O, Et_3N, CH_2Cl_2, room temperature, 14 h; (h) tetrabutylammonium fluoride (TBAF), MeOH, THF, room temperature, 1 h; (i) 1,8-diazabicyclo[5.4.0]undec-7-ene (DBU), *n*-$C_{12}H_{25}SH$, CH_2Cl_2, room temperature, 3 h, 25−46% (three steps from **5**).

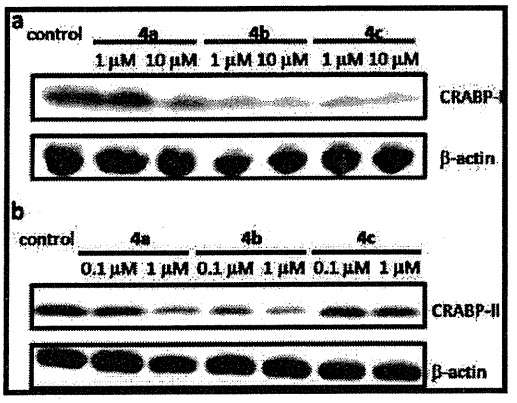

Figure 2. Down-regulation of CRABP-I and CRABP-II by treatment with compounds **4a**−**c**: (a) Western blot detection of CRABP-I levels in MOLT-4 cells after 16 h treatment; (b) Western blot detection of CRABP-II levels in HT1080 cells after 6 h treatment.

the three compounds, though the differences were not large. Compounds **4** also induced a dose-dependent decrease of CRABP-II in HT1080 cells. In this case, **4a** and **4b** strongly reduced the level of CRABP-II (**4b** seemed to be more potent than **4a**), while **4c** was relatively ineffective (Figure 2b). These results suggested that the linker with $n = 2$ is preferable among those investigated. A possible interpretation of this result would be that the structure of compound **4b** is most suitable to bring the ubiquitination sites in CRABPs and the RING domain of cIAP1 into an appropriate spatial relationship for effective ubiquitination to occur. The difference in CRABP-I/II selectivity of **4a** and **4c** suggests that the longer linker is better for down-regulation of CRABP-I, whereas the shorter linker is better for down-regulation of CRABP-II. The differences between CRABP-I and CRABP-II responses to treatment with **4a** and **4c** presumably reflect the structural differences between CRABP-I and -II.

Mechanism of Decrease in CRABPs. We next investigated the mechanism by which CRABPs are downregulated. First, we prepared HT1080 cells expressing FLAG-tagged cIAP1 and examined the influence of **4** on cIAP1 level by Western blot analysis, since esterified analogues of bestatin (**1**) induce autoubiquitination of cIAP1. All the compounds **4a**−**c** showed a dose-dependent cIAP1-decreasing effect, but their efficacy was lower than that of MeBS (**2**) (Figure 3a, Supporting Information, Figure S3). The reason for the weaker activity of **4** compared with MeBS (**2**) is not clear, but it might be due to the bulky ester group or to competing ubiquitination activity toward CRABP-II and cIAP1 itself. A decrease in cIAP1 level was also seen in MOLT-4 cells (Supporting Information, Figure S4).

Next, we pretreated the cells with an excess amount of MeBS (**2**) to investigate whether the reduction of CRABP-II by **4** was mediated by cIAP1 (Figure 3b). The pretreatment with an excess amount of MeBS (**2**) resulted in complete disappearance of cIAP1 but did not influence the CRABP-II level (lane 2). Both CRABP-II and cIAP1 levels were decreased by treatment with **4b** [without pretreatment with MeBS (**2**)] as mentioned above (lane 3). On the other hand, compound **4b** had no effect on CRABP-II levels in cells pretreated with 1000 μM MeBS (**2**) (lane 4). These results indicate that **4b** reduces the CRABP-II

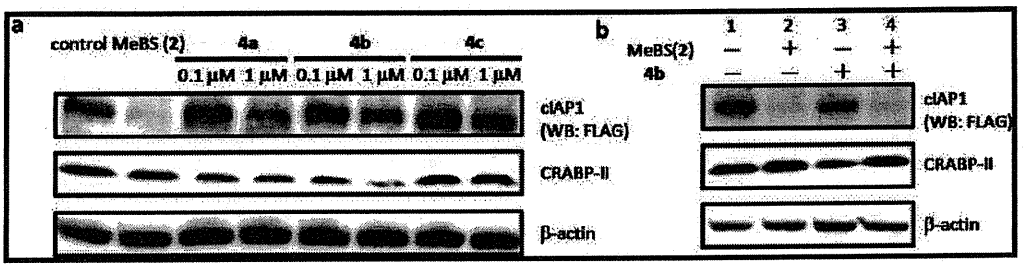

Figure 3. Western blot detection of CRABP-II and cIAP1 levels in HT1080 cells expressing FLAG-tagged cIAP1: (a) CRABP-II and cIAP1 levels after 6 h treatment with **4**; (b) influence of pretreatment of MeBS (**2**) on CRABP-II degradation induction. The cells were treated with 1 μM **4b** for 3 h. MeBS (**2**) (1000 μM) was added to the culture 1 h prior to the addition of **4b**.

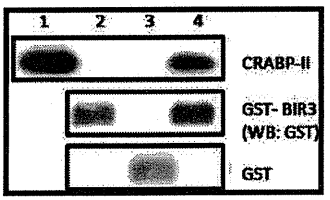

Figure 4. Western blot detection of GST-BIR3, GST, and CRABP-II levels of samples prepared by pull-down assay in vitro: lane 1, CRABP-II levels; lane 2, mixture of GST-BIR3 and CRABP-II; lane 3, mixture of GST, CRABP-II, and **4b**; lane 4, mixture of GST-BIR3, CRABP-II, and **4b**.

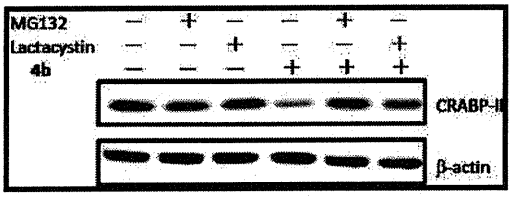

Figure 5. Influence of pretreatment with proteasome inhibitors on CRABP-II degradation induction. Western blot detection of CRABP-II and cIAP1 levels in HT1080 cells expressing FLAG-tagged cIAP1. The cells were treated with 1 μM **4b** for 6 h. MG132 (10 μM) and lactacystin (10 μg/mL) were added to the culture 30 min prior to the addition of **4b**.

level in cIAP1-expressing cells but not in cIAP1-depleted cells, suggesting that cIAP1 mediates the ubiquitination of CRABP-II protein for proteasomal degradation in these cells.

We next examined the formation of a ternary complex consisting of **4b**, cIAP1, and CRABP-II by means of GST pull-down assay using the GST-tagged BIR3 domain of cIAP1, to which MeBS (**2**) binds. As shown in Figure 4, GST-BIR3 coprecipitated CRABP-II in the presence of **4b** (lane 4) but not in the absence of **4b** (lane 2). GST did not pull down CRABP-II even in the presence of **4b** (lane 3). This result indicates that CRABP-II is held in proximity to cIAP1 by **4b**, as we had hoped.

Next, we investigated the influence of proteasome inhibitors on the CRABP-II level in **4b**-treated cells. (Figure 5). The reduction of CRABP-II by **4b** was blocked by proteasome inhibitors MG132 and lactacystin. Thus, the decrease of CRABP-II induced by **4b** can be attributed to proteasomal degradation.

In addition, we confirmed that the decrease in CRABPs was not caused by a partial structure of **4** or by a mere mixture of MeBS (**2**) and ATRA (**3**) (Figure 6). Compound **4b** induced a decrease of CRABP-II, whereas the mixture of MeBS (**2**) and ATRA (**3**) did not. The treatments with 1 μM MeBS (**2**), and the combination of 1 μM MeBS (**2**) and 1 μM ATRA (**3**) decreased the cIAP1 level but did not affect the CRABPs level in HT1080. ATRA (**3**) at 1 μM did not cause any decrease of cIAP1 or CRABP. Similar results were obtained when HT1080

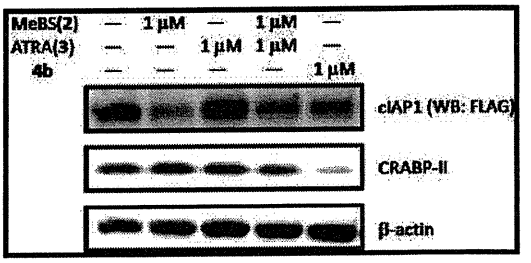

Figure 6. Influence of combination of MeBS (**2**) and ATRA (**3**). Western blot detection of CRABP-II and cIAP1 levels in HT1080 cells expressing FLAG-tagged cIAP1. The cells were treated with 1 μM MeBS (**2**), 1 μM ATRA (**3**), or 1 μM **4b** for 6 h.

or MOLT-4 cells were treated with 10 μM MeBS (**2**) and ATRA (**3**) (Supporting Information, Figure S5). Thus, conjunction of MeBS (**2**) and ATRA (**3**) within a single molecule is essential for CRABP degradation-inducing activity.

It was reported that ATRA (**3**) influences CRABPs levels by transactivation of RAR[23] or that ATRA (**3**) shows effects on HL-60 cell differentiation.[24] However, **4b** did not show agonistic activity toward RARs in reporter gene assay (Supporting Information, Figure S6). Compound **4b** did not show effects on HL-60 cell differentiation or did not enhance cell differentiation induced by ATRA (**3**) (data not shown). Addtionally, **4b** did not induce degradation of RARα (Supporting Information, Figure S7) and did not bind to RARs (Supporting Information, Figure S8). Thus, **4b** showed selective degradation-inducing activity for CRABPs, but not RARα or β-actin, as judged from Western blot experiments with equal loadings of total protein. These results indicated that **4b** has high specificity for degradation of CRABPs. All the results are consistent with our hypothesis that the hybrid molecules **4** form an artificial ternary complex with cIAP1 and CRABP, in which cIAP1 ubiquinates CRABP, leading to its degradation by proteasome.

These small molecules **4** have sufficient membrane permeability and stability to be used in cell systems and are effective in low concentration. Therefore, they might be suitable for a variety of studies in cells and/or animals. In addition, this protein knockdown strategy might be generally adaptable to a wide range of proteins by replacing ATRA (**3**) with a specific ligand for the target protein. Therefore, protein knockdown could be a simple and easy technique to complement genetic ablation at the DNA level (gene knockout) or the mRNA level (gene knockdown).

(23) (a) Aström, A.; Tavakkol, A.; Pettersson, U.; Cromie, M.; Elder, J. T.; Voorhees, J. J. *J. Biol. Chem.* **1991**, *266*, 17662–17666. (b) Geisen, C.; Denk, C.; Gremm, B.; Baust, C.; Karger, A.; Bollag, W.; Schwarz, E. *Cancer Res.* **1997**, *57*, 1460–1467. (c) Dutta, A.; Sen, T.; Banerji, A.; Das, S.; Chatterjee, A. *J. Oncol.* **2009**, *2009*, 627840.

(24) Kim, S. H.; Kim, S. W.; Choi, S. J.; Kim, Y. C.; Kim, T. S. *Bioorg. Med. Chem.* **2006**, *19*, 6752–6757.

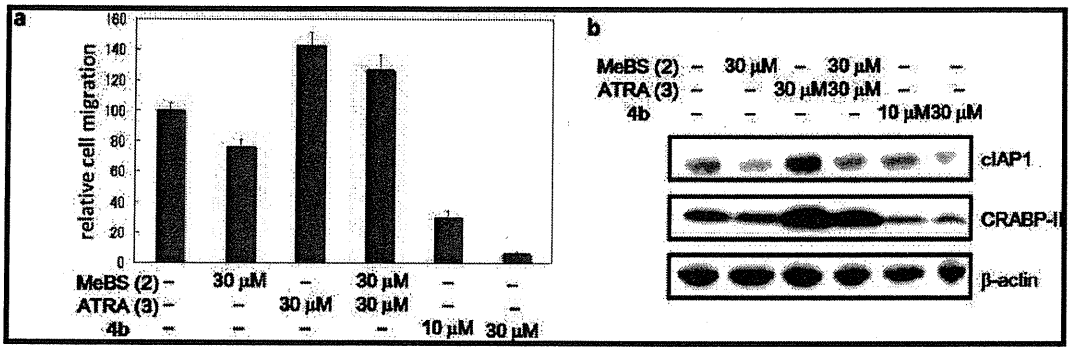

Figure 7. Suppression of cell migration by compound **4b** and degradation of CRABP-II in IMR-32 cells. (a) Relative IMR-32 cell migration. Results are presented as means ± SEM (performed in triplicate). (b) Western blot detection of CRABP-II and cIAP1 levels in IMR-32 cells after 24 h treatment with each reagent.

Inhibitory Activity on Tumor Invasion in Cell-Based Assay. Finally, we tested the effect of **4b** on neuroblastoma cells to explore the potential clinical usefulness of CRABP-II degradation inducers. It has been reported that CRABP-II is closely associated with development of neuroblastoma, Wilms tumor and HNSCC, and a reduction of CRABP-II level suppresses the migration of tumor cells.[15,16] Therefore, we evaluated the migration-suppressing activity of **4b** toward human neuroblastoma IMR-32 cells (Figure 7). Treatment of the IMR-32 cells with 30 μM MeBS (**2**) slightly reduced the cell migration by approximately 30%, in agreement with previous reports that MeBS (**2**) shows antitumor activity.[10a,25] Interestingly, treatment of the cells with ATRA (**3**) alone or the combination of MeBS (**2**) and ATRA (**3**) enhanced the cell migration by 30–40%, possibly as a result of up-regulation of CRABP-II expression by ATRA (**3**). As expected, treatment of the cells with 10 and 30 μM **4b** remarkably reduced the cell migration by approximately 75% and 95%, respectively. Moreover, the extent of migration inhibition was well correlated with the CRABP-II level in the cells. MeBS (**2**) did not affect CRABP-II levels in IMR-32 cells, while ATRA (**3**) or the combination of MeBS (**2**) and ATRA (**3**) up-regulated CRABP-II levels. Since compound **4b** induced degradation of CRABP-II, it might be a useful tool for studying the function(s) of CRABP-II.

Targeted cancer therapy blocks the growth of cancer cells by interfering with specific molecules required for carcinogenesis and tumor growth, rather than by simply interfering with rapid cell division, as is done with traditional chemotherapy.[26] Targeted cancer therapies may be more effective than traditional chemotherapy and less harmful to normal cells. Many kinds of target proteins related to cancer have been identified so far. Further, small-molecular inhibitors for target enzymes or modulators for target receptors have been discovered, and some of them are used for targeted cancer therapy. But many cancer-related proteins, including CRABP-II, can not currently be functionally regulated with small molecules. CRABP-II is expressed in several cancers, including breast cancer,[27] Wilms tumor,[28] HNSCC,[16] ovarian cancer,[29] gastric cancer,[30] uterine leiomyoma,[31] and melphalan- or phorbol-ester-resistant cell lines,[32] suggesting that it may play a role in cancer development. In Wilms tumor, CRABP-II overexpression has been reported to correlate with poor clinical outcome.[15] Here, we found that the small-molecular CRABP-II degradation inducer **4b** inhibited migration of neuroblastoma cells. Thus, CRABP-II degradation inducers may be effective for therapy of neuroblastoma and other CRABP-II-overexpressing cancers. Further studies on various types of cancer cells, including cell proliferation assay, are in progress.

The strategy described in this paper might also be adaptable to a range of cancer-related proteins by replacing ATRA (**3**) with specific ligands for the target proteins. In addition, suppression of cIAP1 function is thought to be favorable for cancer treatment,[33] and disruption of the cIAP1 gene in mice results in no obvious abnormality.[34] Therefore, suppression or degradation of cIAP1, which is overexpressed in several human cancers,[7] should not vitiate the anticancer effect. On the other hand, protacs have utilized peptides recognized by two kinds of E3 ligase complex, von Hippel–Lindau tumor suppressor (VHL), which is deficient or mutated in several cancer,[35] and

(25) Sekine, K.; Fujii, H.; Abe, F.; Nishikawa, K. *Int. J. Cancer.* **2001**, *94*, 485–491.
(26) Schultz, R. M., Ed; *Advances in Targeted Cancer Therapy*; Birkhaeuser: Basel, 2005.
(27) (a) Korkola, J. E.; DeVries, S.; Fridlyand, J.; Hwang, E. S.; Estep, A. L.; Chen, Y. Y.; Chew, K. L.; Dairkee, S. H.; Jensen, R. M.; Waldman, F. M. *Cancer Res.* **2003**, *63*, 7167–7175. (b) Bertucci, F.; Houlgatte, R.; Benziane, A.; Granjeaud, S.; Adélaïde, J.; Tagett, R.; Loriod, B.; Jacquemier, J.; Viens, P.; Jordan, B.; Birnbaum, D.; Nguyen, C. *Hum. Mol. Genet.* **2000**, *9*, 2981–2991.
(28) (a) Li, W.; Kessler, P.; Williams, B. R. *Oncogene* **2005**, *24*, 457–468. (b) Li, C. M.; Guo, M.; Borczuk, A.; Powell, C. A.; Wei, M.; Thaker, H. M.; Friedman, R.; Klein, U.; Tycko, B. *Am. J. Pathol.* **2002**, *160*, 2181–2190.
(29) Hibbs, K.; Skubitz, K. M.; Pambuccian, S. E.; Casey, R. C.; Burleson, K. M.; Oegema, T. R. J.; Thiele, J. J.; Grindle, S. M.; Bliss, R. L.; Skubitz, A. P. *Am. J. Pathol.* **2004**, *165*, 397–414.
(30) Nishigaki, M.; Aoyagi, K.; Danjoh, I.; Fukaya, M.; Yanagihara, K.; Sakamoto, H.; Yoshida, T.; Sasaki, H. *Cancer Res.* **2005**, *65*, 2115–2124.
(31) Tsibris, J. C.; Segars, J.; Coppola, D.; Mane, S.; Wilbanks, G. D.; O'Brien, W. F.; Spellacy, W. N. *Fertil. Steril.* **2002**, *78*, 114–121.
(32) Samuel, S.; Bernstein, L. R. *Mol. Carcinog.* **2004**, *39*, 34–60.
(33) (a) Imoto, I.; Yang, Z. Q.; Pimkhaokham, A.; Tsuda, H.; Shimada, Y.; Imamura, M.; Ohki, M.; Inazawa, J. *Cancer Res.* **2001**, *61*, 6629–6634. (b) Imoto, I.; Tsuda, H.; Hirasawa, A.; Miura, M.; Sakamoto, M.; Hirohashi, S.; Inazawa, J. *Cancer Res.* **2002**, *62*, 4860–4866. (c) Dai, Z.; Zhu, W. G.; Morrison, C. D.; Brena, R. M.; Smiraglia, D. J.; Raval, A.; Wu, Y. Z.; Rush, L. J.; Ross, P.; Molina, J. R.; Otterson, G. A.; Plass, C. *Hum. Mol. Genet.* **2003**, *12*, 791–80. (d) Zender, L.; Spector, M. S.; Xue, W.; Flemming, P.; Cordon-Cardo, C.; Silke, J.; Fan, S. T.; Luk, J. M.; Wigler, M.; Hannon, G. J.; Mu, D.; Lucito, R.; Powers, S.; Lowe, S. W. *Cell* **2006**, *125*, 1253–1267.
(34) Conze, D. B.; Albert, L.; Ferrick, D. A.; Goeddel, D. V.; Yeh, W. C.; Mak, T.; Ashwell, J. D. *Mol. Cell. Biol.* **2005**, *25*, 3348–3356.
(35) (a) Hon, W.; Wilson, M. I.; Harlos, K.; Claridge, T. D. W.; Schofield, C. J.; Pugh, C. W.; Mazwell, P. H.; Ratcliffe, P. J.; Stuart, D. I.; Jones, E. Y. *Nature* **2002**, *417*, 975–978. (b) Kapitsinou, P. P.; Haase, V. H. *Cell Death Differ.* **2008**, *15*, 650–659. (c) Gnarra, J. R.; et al. *Nat. Genet.* **1994**, *7*, 85–90.

β-transducin repeat-containing protein (β-TRCP) Skp1-Cullin-F box (SCF) complex ($SCF^{\beta\text{-TRCP}}$), which plays important roles in many tissues.[36] Those peptide-based protacs, especially those utilizing $SCF^{\beta\text{-TRCP}}$,[4a,b] seem best suited to cell-free systems and might be difficult to use in cancer treatment due to stability issues. Evaluation of our protein degradation inducers, MeBS (**2**)−ligand hybrid molecules, for targeted cancer therapy seems warranted.

Conclusion

We designed and synthesized CRABPs degradation inducers **4**, in which a ligand for CRABPs is conjugated with MeBS (**2**) via a spacer, aiming to make use of the ubiquitin E3 ligase activity of cIAP1. Compounds **4** induced down-regulation of CRABPs in cells. Our results indicate that these small molecules induce the formation of an artificial (nonphysiological) ternary complex of cIAP1 and CRABPs, leading to degradation of CRABPs via the ubiquitin-proteasome pathway. Compound **4b** has sufficient activity, permeability, and stability for use in cellular systems, and we confirmed that it inhibited migration of neuroblastoma IMR-32 cells.

This strategy for protein knockdown should be widely applicable by replacing ATRA (**3**) with specific ligands for other target proteins and should provide a methodology to complement gene knockout and gene knockdown techniques. It is expected to be useful for probing biological functions of proteins and might also be applicable for targeted cancer therapy using MeBS (**2**) conjugated with ligands for cancer-related proteins.

Acknowledgment. The work described in this paper was partially supported by Grants-in-Aid for Scientific Research from The Ministry of Education, Culture, Sports, Science and Technology, Japan, and the Japan Society for the Promotion of Science. We are grateful to Nippon Kayaku Co., especially Dr. Keiko Sekine, for providing bestatin (**1**) and MeBS (**2**), to Dr. Yukihide Tomari, Dr. Tomoko Kawamata, Mr. Shintaro Iwasaki, and Mr. Shinichi Sato for their help with Western blot detection, to Prof. Makoto Makishima with providing RAR plasmids, and to Dr. Tomomi Noguchi-Yachide for HL-60 differentiation assay.

Supporting Information Available: Experimental procedure, copies of ^{1}H NMR spectra, Figures S1−S8, and complete ref 35c. This material is available free of charge via the Internet at http://pubs.acs.org.

JA100691P

(36) Deshaies, R. J. *Annu. Rev. Cell Dev. Biol.* **1999**, *15*, 435–467.

THE JOURNAL OF BIOLOGICAL CHEMISTRY VOL. 285, NO. 21, pp. 16369–16377, May 21, 2010

Binding of PDZ-RhoGEF to ATP-binding Cassette Transporter A1 (ABCA1) Induces Cholesterol Efflux through RhoA Activation and Prevention of Transporter Degradation*[S]

Received for publication, August 31, 2009, and in revised form, March 24, 2010 Published, JBC Papers in Press, March 26, 2010, DOI 10.1074/jbc.M109.061424

Keiichiro Okuhira[‡1], Michael L. Fitzgerald[§], Norimasa Tamehiro[§], Nobumichi Ohoka[‡], Kazuhiro Suzuki[‡], Jun-ichi Sawada[‡], Mikihiko Naito[‡], and Tomoko Nishimaki-Mogami[‡]

From the [‡]National Institute of Health Sciences, 1-18-1, Kamiyoga, Setagaya-ku, Tokyo 158-8511, Japan and the [§]Lipid Metabolism Unit and Center for Computational and Integrative Biology, Massachusetts General Hospital, Harvard Medical School, Boston, Massachusetts 02114

ATP-binding cassette transporter A1 (ABCA1)-mediated lipid efflux to apolipoprotein A1 (apoA-I) initiates the biogenesis of high density lipoprotein. Here we show that the Rho guanine nucleotide exchange factors PDZ-RhoGEF and LARG bind to the C terminus of ABCA1 by a PDZ-PDZ interaction and prevent ABCA1 protein degradation by activating RhoA. ABCA1 is a protein with a short half-life, and apoA-I stabilizes ABCA1 protein; however, depletion of PDZ-RhoGEF/LARG by RNA interference suppressed the apoA-I stabilization of ABCA1 protein in human primary fibroblasts. Exogenous PDZ-RhoGEF expression activated RhoA and increased ABCA1 protein levels and cholesterol efflux activity. Likewise, forced expression of a constitutively active RhoA mutant significantly increased ABCA1 protein levels, whereas a dominant negative RhoA mutant decreased them. The constitutively active RhoA retarded ABCA1 degradation, thus accounting for its ability to increase ABCA1 protein. Moreover, stimulation with apoA-I transiently activated RhoA, and the pharmacological inhibition of RhoA or the dominant negative RhoA blocked the ability of apoA-I to stabilize ABCA1. Finally, depletion of RhoA or RhoGEFs/RhoA reduces the cholesterol efflux when transcriptional regulation via PPARγ is eliminated. Taken together, our results have identified a novel physical and functional interaction between ABCA1 and PDZ-RhoGEF/LARG, which activates RhoA, resulting in ABCA1 stabilization and cholesterol efflux activity.

Homeostasis of cellular cholesterol is critical for human physiology, and disturbance of the regulatory processes that maintain cholesterol homeostasis can cause cardiovascular disease (1, 2). In particular, high density lipoprotein (HDL)[2] cholesterol levels are inversely correlated with coronary heart disease risk in humans and in animal models, and HDL elevation decreases formation and progression of foam cell lesions (3, 4). ATP-binding cassette transporter A1 (ABCA1) mediates the active transfer of excess cholesterol from cells to extracellular apolipoproteins, primarily apolipoprotein A-I (apoA-I), to form nascent HDL particles. The physiological importance of this cholesterol efflux is clearly demonstrated in patients with Tangier disease, a rare genetic condition caused by loss-of-function mutations in ABCA1 that is characterized by a near absence of HDL and a massive deposition of cholesterol esters in peripheral tissues (5–7).

The activity of ABCA1 is regulated both at the transcriptional level and at the post-translational level. We and others have shown that a complex network of protein-protein interactions mediates the post-translational regulation of ABCA1 (8–13). In particular, ABCA1 contains a PDZ protein-binding motif located in the terminal four residues of the cytoplasmic tail of the transporter, and we have previously identified that the PDZ protein β1-syntrophin bound ABCA1 through this motif (8). The ABCA1/β1-syntrophin interaction increased cholesterol efflux by increasing the cell surface expression of ABCA1 and protecting it from degradation. In addition, we also identified that a subunit of the serine palmitoyltransferase enzyme, SPTLC1 (serine palmitoyltransferase long chain base subunit 1), was associated with ABCA1, and this interaction reduced the ABCA1 activity by trapping ABCA1 in the endoplasmic reticulum (9).

Here we show that PDZ-RhoGEF (Rho guanine nucleotide exchange factor 11) and leukemia-associated RhoGEF (LARG, Rho guanine nucleotide exchange factor 12) bind ABCA1 and regulate ABCA1 protein levels and cholesterol efflux activity. The RhoGEFs are known to control the activation of Rho GTPases by stimulating the exchange of GDP for GTP (14, 15). Members of the RhoGEF family have a Dbl homology (DH) domain and a pleckstrin homology (PH) domain that are responsible for the guanine nucleotide exchange factor activity. PDZ-RhoGEF and LARG, together with p115-RhoGEF, consti-

* This work was supported by National Institutes of Health Grant HL-074136 (to M. L. F.). This work was also supported by grants-in-aid for scientific research from the Japan Society for the Promotion of Science, by a research fund from Japan Health Sciences Foundation, by a Takeda Science Foundation grant (to K. O.), and by American Heart Association Grant 09GRNT2260352 (to M. L. F.).

[S] The on-line version of this article (available at http://www.jbc.org) contains supplemental Fig. S1.

[1] To whom correspondence should be addressed: National Institute of Health Sciences, 1-18-1, Kamiyoga, Setagaya-ku, Tokyo 158-8511, Japan. Tel.: 81-3-3700-9478; Fax: 81-3-3707-6950; E-mail: okuhira@nihs.go.jp.

[2] The abbreviations used are: HDL, high density lipoprotein; ABCA1, ATP-binding cassette transporter subfamily A member 1; apoA-I, apolipoprotein A-I; PMA, phorbol 12-myristate 13-acetate; DH, Dbl homology; PH, pleckstrin homology; IGF, insulin-like growth factor; HA, hemagglutinin; EGFP, enhanced green fluorescent protein; RFP, red fluorescence protein; siRNA, small interfering RNA; CA, constitutively active; DN, dominant negative; PPAR, peroxisome proliferator-activated receptor.

tute a unique subfamily of RhoGEFs characterized by the presence of a regulator of G protein signaling domain, and their guanine nucleotide exchange factor activity is specific for RhoA compared with Rac1 and Cdc42 (16–22). PDZ-RhoGEF and LARG, but not p115-RhoGEF, both have an N-terminal PDZ domain, which allows them to associate with transmembrane proteins or receptors including Plexin-B1 (23–27), insulin-like growth factor (IGF-1) receptor (28), lysophophatidic acid receptor (29), and CD44 (30). Through these interactions PDZ-RhoGEF and LARG couple extracellular signaling processes to the activation of RhoA. Thus, the PDZ-RhoGEF and LARG interaction to ABCA1 implies that 1) ABCA1 may act not only as a lipid transporter but may also act as a receptor for RhoA signaling and 2) RhoA may regulate the activity and expression of ABCA1 protein.

In this report, we have examined the functional significance of the interaction of PDZ-RhoGEF/LARG to ABCA1 on the activity of cholesterol efflux and ABCA1 regulation. Our results suggest a mechanism by which the ABCA1/PDZ-RhoGEF complex couples the binding of apoA-I to ABCA1 to the activation of RhoA and the subsequent inhibition of ABCA1 protein turnover.

EXPERIMENTAL PROCEDURES

Materials—The following reagents were purchased from the indicated suppliers: mouse monoclonal anti-Myc antibody (4A6) (Upstate); rabbit anti-HA (Clontech); Alexa Fluor 555 goat anti-mouse IgG, Lipofectamine 2000 (Invitrogen); M2 anti-FLAG mouse monoclonal agarose-conjugated antibody, mouse anti-β-actin antibody, protease inhibitor mixture, and cycloheximide (Sigma); mouse anti-GTRAP48 (rat PDZ-RhoGEF) (BD Biosciences); mouse monoclonal anti-ABCA1 (Abcam); rabbit polyclonal anti-ABCA1 antibody (Affinity Bioreagents); mouse monoclonal anti-RhoA, cell-permeable C3-transferase, and Rho activation assay biochemistry kit (Cytoskeleton Inc., Denver, CO); anti-calnexin (StressGen Biotechnologies); SMARTpool siRNA duplexes (Dharmacon); apoA-I (Intracell); radionucleotides (PerkinElmer Life Sciences); human dermal fibroblast Nucleofector kit (Amaxa); and TrueBlot anti-rabbit Ig IP beads (eBioscience).

DNA Constructs—The FLAG-tagged ABCA1 and β1-syntrophin constructs have been previously described (31, 32). The cDNA of full-length PDZ-RhoGEF (KIAA0380) was kindly provided by Takahiro Nagase (Kazusa DNA Research Institute). To create the ΔDH/PH mutant of PDZ-RhoGEF cDNA, full-length PDZ-RhoGEF cDNA was digested with EcoNI (there are two cutting sites at either ends of the sequence coding the tandem of DH and PH domain), and the backbone vector was self-ligated. The cDNA coding for human RhoA was amplified by reverse transcription-PCR from total RNA isolated from HeLa cell line. The T19N and Q63L mutants of RhoA were generated by site-directed PCR mutagenesis. The cDNAs were subcloned into pCMV-Tag3 (Stratagene) or pCMV-HA (Clontech) to produce Myc- or HA-tagged versions, respectively. Enhanced green fluorescent protein (EGFP) or red fluorescence protein (RFP) was fused at the N terminus of ABCA1 or PDZ-RhoGEF in pcDNA3.1 backbone. The correct DNA sequences of all constructs were confirmed by DNA sequencing.

Cell Culture—HEK293 cells were maintained in Dulbecco's modified Eagle's medium containing 10% fetal bovine serum. The cDNA transfections were performed using Lipofectamine 2000 reagent. THP-1 cells were maintained RPMI medium containing 10% fetal bovine serum. Differentiation of THP-1 cells was induced by phorbol 12-myristate 13-acetate (PMA) for 72 h. The differentiated cells were cultured in RPMI medium containing 0.2% bovine serum albumin for 24 h and then used for the experiments (33). Primary human dermal fibroblasts (NHDF-Neo, CC-2509) were purchased from Lonza (Walkersville, MD). The cells were maintained in FGM-2 medium with provided supplement (Lonza).

Overlay Assays—The interaction of the ABCA1 or ABCA7 C terminus with the PDZ domains of PDZ-RhoGEF or LARG was analyzed using a biotinylated peptide representing the final 20 amino acids of the ABCA1 (Bio-VDVAVLTSFLQDEKVKESYV) or ABCA7 (Bio-QHPKRVSRFLEDPSSVETVI). The PDZ array membrane (Panomics TransSignal™ PDZ Domain Array IV) that includes affinity purified PDZ domains of PDZ-RhoGEF (GEF11) and LARG (GEF12) spotted in duplicate (total 34 PDZ domains from 24 proteins) were blocked overnight in blocking buffer at 4 °C with gentle agitation. 15 μl of the peptides (50 μM) were mixed with 15 μl of NeutrAvidin-horseradish peroxidase (1 mg/ml; Pierce) for 30 min at 4 °C and diluted into 5 ml of 1× blocking buffer and incubated with the arrays for 2 h at room temperature (final peptide concentration, 150 nM). After washing, the binding of the peptides was detected with enhanced chemiluminescence and quantitated using an Alpha Innotech FluorChem 8800 imager. The binding of full-length PDZ-RhoGEF to the ABCA1 C terminus was determined using the overlay technique as previously described (8). In brief, equal amounts of purified His-tagged bacterial polypeptides representing the last 185 amino acids of ABCA1, with or without the PDZ motif (wild type, Δ4), were separated by SDS-PAGE and transferred to nitrocellulose. Blocked membranes (5% dried milk proteins, 1% bovine serum albumin, 1× phosphate-buffered saline, overnight at 40 °C) were incubated with 200 mg of a total cellular lysates diluted in 20 ml of blocking buffer. The lysates were obtained from 293-EBNA-T cells transfected with cDNA of HA-tagged versions of full-length PDZ-RhoGEF for 2 h at room temperature. After washing (1× phosphate-buffered saline, 0.1% Tween 20), binding of the PDZ-RhoGEF was detected using an anti-HA monoclonal antibody. The gels run in parallel and Coomassie-stained were used to demonstrate equal loading of the wild type and PDZ motif-deleted His-tagged polypeptides.

Immunoprecipitations—cDNA-transfected 293 cells or primary human fibroblasts were lysed in immunoprecipitation buffer (1% Triton X-100, 50 mM HEPES, pH 7.0, 140 mM NaCl, 3 mM $MgCl_2$, 10% glycerol, and 1% protease inhibitor mixture). The lysates were clarified by centrifugation, and ABCA1 interacting proteins complexes were co-precipitated with anti-FLAG M2 monoclonal antibody agarose. For the analysis of protein interactions in primary human fibroblasts, clarified lysates were incubated with rabbit anti-ABCA1 antibody (Affinity Bioreagents). Immunocomplexes were captured with

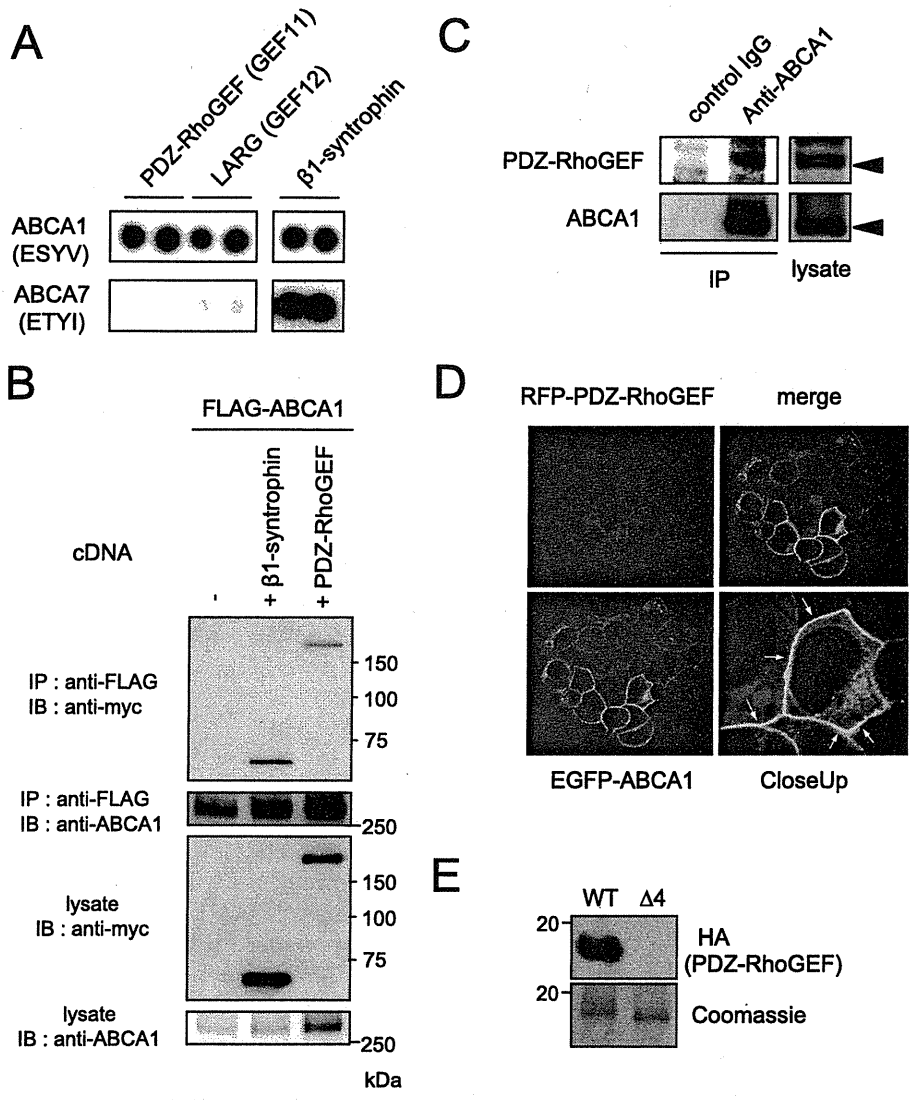

FIGURE 1. **ABCA1 and PDZ-RhoGEF interact in a cellular context in a manner that requires the ABCA1 C-terminal PDZ-binding motif.** *A*, biotinylated peptides representing the ABCA1 or ABCA7 C termini were used to probe against PDZ domains of PDZ-RhoGEF (GEF11), LARG (GEF12), or β1-syntrophin spotted in duplicate. Binding was detected with avidin-horseradish peroxidase. *B*, co-precipitation of ABCA1 and PDZ-RhoGEF. 293 cells were co-transfected with FLAG-tagged ABCA1 and either vector, Myc-tagged β1-syntrophin, or PDZ-RhoGEF. The cells were lysed and ABCA1 was immunoprecipitated with anti-FLAG antibody. Shown are Western blots of lysates or immunoprecipitated samples stained with the indicated antibodies. *C*, the endogenous PDZ-RhoGEF interacts with the endogenous ABCA1 in primary human fibroblasts. Cellular ABCA1 expression was stimulated by LXR and RXR ligands. ABCA1 was immunoprecipitated with anti-ABCA1 antibody. Shown are Western blots of lysates or immunoprecipitated samples stained with the indicated antibodies. *D*, co-localization of EGFP-tagged ABCA1 and RFP-tagged PDZ-RhoGEF in 293 cells. *E*, purified His-tagged polypeptides representing the wild-type ABCA1 C terminus with (*WT*) and without the PDZ motif (Δ4) were separated by SDS-PAGE and transferred to nitrocellulose. The membrane was incubated with lysates expressing HA-tagged PDZ-RhoGEF, and binding was detected using an anti-HA antibody. Coomassie-stained gels run in parallel show equal loading of the ABCA1 peptides. *IB*, immunoblotting; *IP*, immunoprecipitation.

TrueBlot anti-rabbit Ig beads and then analyzed by SDS-PAGE and immunoblotting using the indicated antibodies.

Immunofluorescence—Tet-on 293 cells that inducibly expressing EGFP-tagged ABCA1 were generated (Flp-In™ T-REx™; Invitrogen). RFP-tagged PDZ-RhoGEF was transiently transfected by LF2000 in cells where EGFP-ABCA1 expression was induced by doxycycline. The cells were grown on coverslips and visualized using confocal microscopy (LSM5 510 META; Zeiss).

Cholesterol Efflux Assays—Cholesterol efflux was measured as previously described (34). In brief, 293 cells were seeded into 24-well poly-D-lysine-coated tissue culture plates and were transfected in triplicate with empty vector or the indicated cDNAs using LF2000. Primary human fibroblasts were transfected with a siRNA pool of four duplex (Dharmacon). The siRNA transfection was performed by nucleofection using a human dermal fibroblast Nucleofector kit (Amaxa Biosystems, Cologne, Germany) according to the manufacturer's protocols. After 24 h of transfection, the cells were incubated in culture medium containing 0.5 μCi/ml [^{3}H]cholesterol for 24 h. The cells were equilibrated in containing 2 mg/ml fatty acid-free bovine serum albumin and then incubated with or without 10 μg/ml apoA-I for 20 h (293) or 6 h (primary human fibroblasts). The medium was collected and cleared of cellular debris by an 800 × *g* spin for 10 min, the cell layers were dissolved in 0.1 N NaOH, and the percentage of cholesterol efflux was calculated by scintillation counting.

Determination of Activated RhoA—RhoA activation was determined using a Rho activation assay biochemistry kit (Cytoskelton) according to the provided protocol. Briefly, the cells were incubated in serum-free medium for 3 h and then lysed, GTP-bound RhoA was precipitated with Rhotekin-RBD beads, and immunoprecipitated RhoA was detected by immunoblotting using anti-HA antibody or anti-RhoA antibody. For the experiments of the stimulation with apoA-I, 10 μg/ml of apoA-I was added to cells for indicated times after the 3-h serum-free incubation period.

ABCA1 Degradation—293 cells were transfected with ABCA1 and either cDNAs for wild type RhoA, RhoA-CA, RhoA-DN, or empty vector. At 24 h after transfection, cycloheximide (100 μg/ml) was added to block protein synthesis. The amount of ABCA1 in cell lysate was measured by immunoblotting using anti-ABCA1 antibody after the indicated times. The detected signal was directly quantitated on a LAS-3000 imager (Fujifilm).

ABCA1 Stabilization by ApoA-I—PMA-differentiated THP-1 cells were treated with cell-permeable C3-transferase (2 μg/

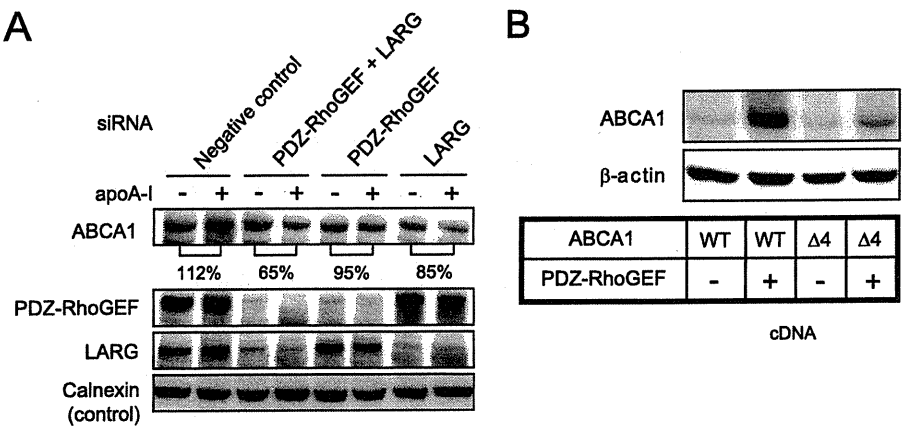

FIGURE 2. **PDZ-RhoGEF/LARG is associated with the increase of ABCA1 protein levels.** *A*, knockdown of RhoGEF expression by siRNA suppressed the apoA-I-mediated ABCA1 stabilization in primary human fibroblast. The cells were transfected with either a nontargeting pool of siRNA duplexes (negative control), siRNA duplex targeting PDZ-RhoGEF, or LARG, or a mixture of siRNA duplexes targeting both PDZ-RhoGEF and LARG. After 48 h transfection, the cells were incubated with apoA-I for 1 h. The level of ABCA1 protein was quantified using a LAS-3000 imager. *B*, PDZ-RhoGEF expression increased ABCA1 protein level in cells expressing wild-type (*WT*) ABCA1 but in cells expressing the ABCA1-Δ4 mutant, which disrupts the ABCA1 PDZ-binding motif. 293 cells were transfected with wild-type or Δ4 mutant of ABCA1 cDNA either alone or together with PDZ-RhoGEF cDNA. The results are representatives of two or more experiments.

ml) for 4 h and then incubated with apoA-I (100 μg/ml) for 1 h. The siRNA-transfected primary human fibroblasts were incubated with 10 μg/ml apoA-I for 1 h. The cDNA-transfected 293 cells were incubated with cycloheximide in the presence or absence of apoA-I for 4 h. The expression of proteins was detected by indicated antibodies and quantitated on a LAS-3000 imager.

RNA Extraction and Quantitative Real-time PCR—Total RNA was isolated using the RNeasy Mini kit according to the provided protocol (Qiagen). Quantitative real-time RT-PCR was performed in an ABI PRISM 7000 sequence detection system using the one-step RT-PCR Master Mix reagent kit (Applied Biosystems). The ABCA1 primers and probe used were: forward primer, 5′-AGGTTTGGAGATGGTTATA-CAATAGTTG-3′; reverse primer, 5′-CTTTTAGGACA-CTTCCCGGAAA-3′; and probe, 5′-FAM-ACGAATAG-CAGGCTCCAACCCTGACC-TAMRA-3′. The data were normalized for 18 S rRNA levels and were presented as fold change compared with normalized ABCA1 message levels in the control cells.

Statistical Analysis—Data from cholesterol efflux assays were found to have equal variance and were further compared by a two-tailed Student's *t* test. Statistical significance were defined by a p of <0.05.

RESULTS

ABCA1 Interacts with PDZ-RhoGEF and LARG—ABCA1 has a highly conserved 46-amino acid C-terminal domain, which resides in the cytoplasmic space and is essential for ABCA1 to bind and transfer lipid to its efflux acceptor apoA-I (31). The final four residues of this domain conform to a type I PDZ protein interaction motif, and we have used mass spectrometry and PDZ protein arrays to screen for proteins that interact with this domain (8). Along with syntrophins these screens indicate PDZ-RhoGEF and LARG may also bind ABCA1 through this motif (8). To further investigate the specificity of the PDZ-RhoGEF and LARG interactions, we used 20-mer biotinylated peptides representing the C terminus of ABCA7, which is a close homologue of ABCA1 (35–38), to probe membranes that had been spotted in duplicate with recombinant proteins of PDZ domains from PDZ-RhoGEF, LARG, and β1-syntrophin expressed in *Escherichia coli*. The ABCA1 peptide strongly interacted with all the three PDZ domains, whereas the ABCA7 peptide bound PDZ domain from β1-syntrophin but not those from PDZ-RhoGEF and LARG (Fig. 1*A*), indicating the PDZ domains of PDZ-RhoGEF and LARG specifically bound the ABCA1 C terminus. To investigate whether ABCA1 physically interacts with PDZ-RhoGEF or LARG in a cellular context, we performed immunoprecipitations in cDNA-transfected HEK293 cells. The PDZ-RhoGEF co-precipitated ABCA1, as did β1-syntrophin (Fig. 1*B*, *top panel*). A similar interaction was also observed between LARG and ABCA1 (data not shown). Significantly, in these assays PDZ-RhoGEF showed a greater potency than β1-syntrophin to enhance the ABCA1 protein levels (Fig. 1*B*, *bottom panel*). We then tested whether endogenous ABCA1 interacts with endogenous PDZ-RhoGEF in primary human fibroblasts, which have been extensively used in studies of ABCA1 function in patients with Tangier disease (39, 40). As shown in Fig. 1*C*, PDZ-RhoGEF in the primary fibroblasts co-precipitated ABCA1, indicating that ABCA1 and PDZ-RhoGEF form a complex in primary cells at endogenous protein expression levels. Next we observed the subcellular localization of ABCA1 and PDZ-RhoGEF by confocal microscopy. In cells expressing EGFP-tagged ABCA1 and RFP-tagged PDZ-RhoGEF, the proteins prominently co-localized at the cell surface (Fig. 1*D*, *white arrows*). To examine the role of the PDZ-binding motif in the interaction between the ABCA1 C terminus and PDZ-RhoGEF, we performed an overlay assay using purified His-tagged bacterial polypeptides representing the last 185 amino acids of the wild type ABCA1 C terminus or a truncated mutant lacking the PDZ-binding motif (Δ4). After SDS-PAGE and transferring these peptides to nitrocellulose, the resulting membranes were incubated with a lysate from 293-EBNA-T cells expressing the full-length HA-tagged PDZ-RhoGEF. PDZ-RhoGEF bound the wild type ABCA1 polypeptide but not the polypeptide lacking the PDZ-binding motif as determined by immunoblotting with anti-HA antibody (Fig. 1*E*, *upper panel*). Gels run in parallel and stained for total protein demonstrated the failure of PDZ-RhoGEF to bind the ABCA1-Δ4 polypeptide was not due to a loading artifact (Fig. 1*E*, *lower panel*). In aggregate these experiments showed that the ABCA1/PDZ-RhoGEF complex can be detected in primary cells at physiological expression levels and that the PDZ domain

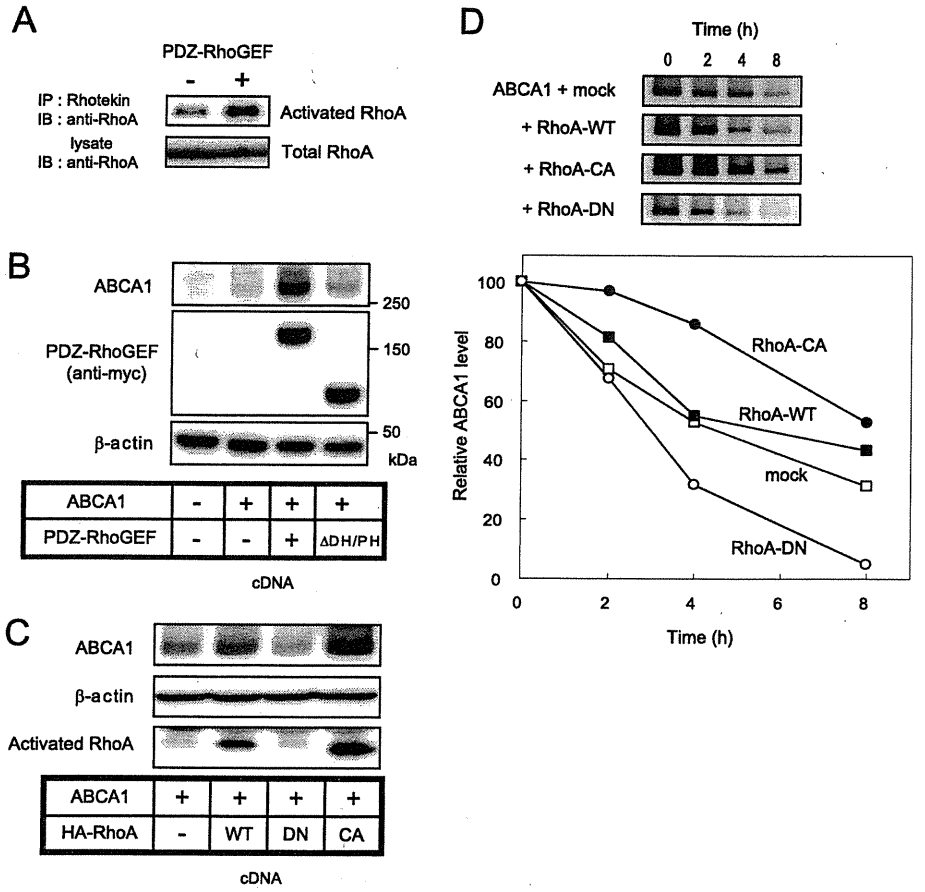

FIGURE 3. **RhoA activation by PDZ-RhoGEF increase the ABCA1 protein levels by blocking its degradation.** *A*, the expression of PDZ-RhoGEF increases the amount of activated RhoA. The transfected cells were lysed, and activated RhoA was precipitated with Rhotekin-RBD beads. Precipitates or lysates were immunoblotted with anti-RhoA to detect activated and total RhoA, respectively. *B*, the ability of PDZ-RhoGEF to enhance ABCA1 expression was attenuated in cells expressing PDZ-RhoGEF ΔDH/PH mutant. 293 cells were transfected with vector alone, ABCA1 cDNA alone, or ABCA1 cDNA together with PDZ-RhoGEF cDNA or PDZ-RhoGEF cDNA mutant lacking the DH and PH domain (ΔDH/PH). *C*, RhoA directly regulates ABCA1 protein expression. The cells were co-transfected with ABCA1 and either HA-tagged wild-type RhoA (*WT*), a dominant negative form of RhoA (*DN*), a constitutively active form of RhoA (*CA*), or with empty vector. The results in *A–C* are representative of two or more experiments. *D*, activated RhoA blocks, and inactivated RhoA enhances the ABCA1 degradation. The cells were co-transfected with ABCA1 and wild-type RhoA, RhoA-CA, RhoA-DN, or empty vector. Cycloheximide was added to block protein synthesis 24 h after transfection. The cells were lysed after the indicated times, and the lysates were immunoblotted with anti-ABCA1 antibody. Shown are representative images, and graphed are the average values expressed as percentage of increase of the amount of ABCA1 quantified by LAS-3000 imager in two (mock and RhoA-DN) or three (wild type RhoA and RhoA-CA) separate experiments. *IB*, immunoblotting; *IP*, immunoprecipitation.

of PDZ-RhoGEF directly interacts with the ABCA1 C-terminal PDZ-binding motif.

PDZ-RhoGEF/LARG Increases ABCA1 Protein Levels—The binding of apoA-I to ABCA1 increases the ABCA1 protein levels by protecting it from calpain-mediated degradation (33, 41). To study the role of PDZ-RhoGEF/LARG in the apoA-I-mediated ABCA1 stabilization, we experimentally down-regulated PDZ-RhoGEF and/or LARG in primary human fibroblasts. We found that the knockdown of these proteins disrupted the ability of apoA-I to increase ABCA1 protein expression (Fig. 2*A*). Conversely, co-transfection of PDZ-RhoGEF with ABCA1 in 293 cells significantly increased the ABCA1 protein level (Fig. 2*B*), whereas the ability of PDZ-RhoGEF to enhance ABCA1 protein level was greatly attenuated in cells expressing the Δ4 mutant of ABCA1 (Fig. 2*B*). ABCA1 protein levels correlate well with cholesterol efflux activity (supplemental Fig. S1*A*). These results indicate that the binding of PDZ-RhoGEF/LARG to ABCA1 results in increased ABCA1 protein levels.

RhoA Activation Is Required for PDZ-RhoGEF-mediated Up-regulation of ABCA1 Protein Levels—PDZ-RhoGEF facilitates the GDP/GTP exchange to activate RhoA (14, 15). Therefore, we tested whether RhoA was activated in PDZ-RhoGEF-transfected cells. As shown in Fig. 3*A*, PDZ-RhoGEF expression increased the amount of activated RhoA without changing total RhoA levels. Next, we used a PDZ-RhoGEF mutant lacking the DH and PH domain (ΔDH/PH), which does not have GEF activity. The ability of PDZ-RhoGEF to enhance ABCA1 expression was greatly attenuated in cells expressing the PDZ-RhoGEF mutant (Fig. 3*B*, Δ*DH/PH*). The efflux activity was reduced as well (supplemental Fig. S1*B*, Δ*DH/PH*). This suggests that the enhancement of the ABCA1 protein level by PDZ-RhoGEF is through a mechanism that activates RhoA. To further investigate whether RhoA activation contributed to the up-regulation of ABCA1, the ABCA1 protein levels were assessed in cells co-expressing ABCA1 and either wild-type RhoA, constitutively active RhoA, dominant negative RhoA, or empty vector. Wild-type RhoA, and more prominently the constitutively active RhoA (HA-RhoA-Q63L, CA), increased the ABCA1 protein level, whereas the dominant negative RhoA (HA-RhoA-T19N, DN) decreased the level of ABCA1 (Fig. 3*C*). These data indicate that RhoA activation is required for the up-regulation of ABCA1 protein levels mediated by PDZ-RhoGEF.

To investigate whether the activated RhoA increases ABCA1 protein levels by reducing its degradation, ABCA1 protein turnover was monitored. After the addition of cycloheximide to block protein synthesis, ABCA1 protein levels were quantified by immunoblots (Fig. 3*D*). In cells expressing empty vector, ABCA1 protein was degraded with a short half-life (~4–5 h), indicating that ABCA1 protein turns over rapidly in 293 cells. In cells expressing wild-type RhoA, ABCA1 decreased by 45% after 4 h of cycloheximide treatment, and that in RhoA-CA cells decreased by 14%, showing that the turnover of ABCA1 was markedly delayed in cells expressing RhoA-CA. On the other

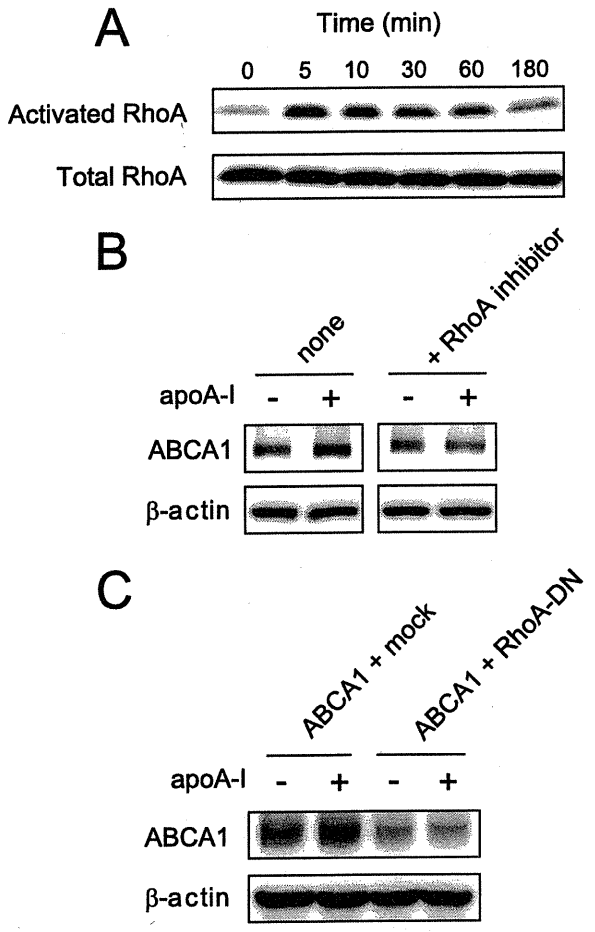

FIGURE 4. **ApoA-I-mediated activation of RhoA is critical for ABCA1 protein stabilization.** *A*, apoA-I transiently activates RhoA. PMA-differentiated THP-1 cells were incubated with apoA-I for indicated times. Shown are immunoblots of lysates (total RhoA) or immunoprecipitated samples (activated RhoA) stained with anti-RhoA antibody. *B*, RhoA selective inhibitor, exoenzyme C3 transferase, abolishes the apoA-I-mediated stabilization of ABCA1. PMA-differentiated THP-1 cells were incubated with apoA-I for 1 h. Prior to adding apoA-I, the cells were pretreated with exoenzyme C3 transferase for 4 h or not. *C*, the ability of apoA-I to stabilize ABCA1 protein is lost in cells expressing RhoA-DN. The cells were co-transfected with ABCA1 and either empty vector or RhoA-DN. The cells were incubated with cycloheximide in the presence or absence of apoA-I for 4 h. The results are representative of two or more experiments.

hand, ABCA1 level in cells expressing RhoA-DN decreased by 95% at 8 h, whereas more than 40% of ABCA1 still remained in cells expressing wild-type RhoA, thus indicating that ABCA1 turnover was facilitated in cells expressing RhoA-DN. This result indicates that activation of RhoA prevents, and inactivation of RhoA enhances, the degradation of the ABCA1 protein.

We further investigated the role of RhoA in the apoA-I-mediated ABCA1 up-regulation. apoA-I caused a rapid (peak at 5 min) and transient activation of RhoA in PMA-differentiated THP-1 macrophages (Fig. 4*A*). In THP-1 cells, the addition of apoA-I led to a stabilization of ABCA1 protein as previously reported (33, 41), and this effect was impaired by pretreatment with exoenzyme C3 transferase, a RhoA selective inhibitor (Fig. 4*B*). In 293 cells transfected with ABCA1, apoA-I increased the ABCA1 expression, whereas the co-expression of RhoA-DN abolished the ability of apoA-I to increase ABCA1 (Fig. 4*C*). Thus, apoA-I activates RhoA, and the RhoA activation is required for the apoA-I-mediated stabilization of ABCA1. Collectively, these results indicate that the apoA-I binding and stabilization of ABCA1 is associated with the activation of RhoA, which depends upon the interaction between PDZ-RhoGEF/LARG and ABCA1 C terminus.

Prolonged Inhibition of RhoA Induces ABCA1 mRNA Expression—In contrast to our results that the transitory activation of RhoA by apoA-I positively regulates ABCA1 protein expression, RhoA inactivation by inhibitors or siRNA results in an increased expression of ABCA1 mRNA by a mechanism that depends on the activity of the nuclear hormone receptor called peroxisome proliferator-activated receptor γ (PPARγ), which is considered to be another mechanism to regulate ABCA1 expression by the activity of RhoA (42, 43). Indeed, we confirmed that ABCA1 mRNA was significantly increased in PMA-differentiated macrophages in which RhoA was inhibited by exoenzyme C3 transferase for 24 h (Fig. 5*A*). We also examined whether the ABCA1 mRNA expression was increased in the cells treated with siRNAs against RhoGEFs (PDZ-RhoGEF + LARG) and/or RhoA. RhoGEFs siRNA transfection slightly increased the ABCA1 mRNA level, and RhoA or RhoGEF/RhoA (PDZ-RhoGEF + LARG + RhoA) siRNA transfection significantly increased it (Fig. 5*B*, *gray bars*). Consistent with the increase of ABCA1 mRNA induced by RhoA inhibition being dependent PPARγ activity, the stimulation of ABCA1 mRNA by silencing of RhoA was attenuated when the expression of PPARγ was simultaneously suppressed (Fig. 5*B*, *black bar*). These results indicate that RhoA activation leads to ABCA1 protein stabilization; however, prolonged RhoA inactivation causes the up-regulation of the ABCA1 mRNA levels via PPARγ, indicating two opposing mechanisms that modulate ABCA1 expression by RhoA.

RhoGEF or RhoGEF/RhoA Silencing Decreases the Efflux Activity in PPARγ-depleted Cells—Finally, we examined cholesterol efflux activity in the cells treated with siRNA against RhoGEFs and RhoA. Because the prolonged inactivation by silencing RhoA results in up-regulation of ABCA1 mRNA via PPARγ (Fig. 5*B*), we measured the cholesterol efflux in the cells in which PPARγ was co-silenced to block the ABCA1 mRNA up-regulation to deconvolute these two opposing effects on ABCA1 expression. Consistent with the down-regulation of ABCA1 protein level (Fig. 2A), silencing of RhoGEFs significantly, and co-silencing of RhoGEFs/RhoA more markedly, reduced the cholesterol efflux mediated by ABCA1 (Fig. 6, *black bars*). The reduction of cholesterol efflux activity by silencing RhoGEFs/RhoA was not observed when PPARγ expression remained intact (Fig. 6, *gray bars*). This indicates that in the absence of PPARγ activity, the loss of RhoA activation and the subsequent stabilization of the ABCA1 protein level significantly reduces ABCA1 efflux activity to apoA-I.

DISCUSSION

Accumulating evidence suggests that protein-protein interactions in a network play significant roles in regulating ABCA1 activity (8–13). Here we show that PDZ-RhoGEF physically and functionally interacts with ABCA1. The C terminus of ABCA1 contains a strongly conserved type I PDZ-binding motif, and this

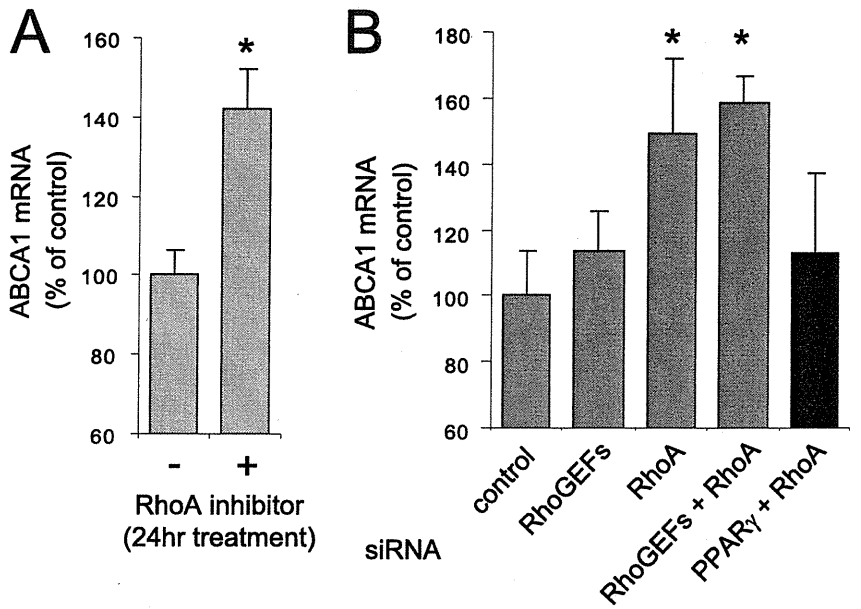

FIGURE 5. **Inhibition of RhoA signaling causes an increase in ABCA1 mRNA.** *A*, RhoA inhibition by exoenzyme C3 transferase increased the ABCA1 mRNA in PMA-differentiated THP-1 macrophages. The cells were treated with exoenzyme C3 transferase for 24 h. mRNA was extracted and measured by the quantitative reverse transcription-PCR. Ratios of the ABCA1 to 18 S transcripts are expressed as percentages of the control treated cells. *B*, primary human fibroblasts were transfected with either a nontargeting pool of siRNA duplexes (control) or with siRNA duplexes targeting RhoGEFs (PDZ-RhoGEF + LARG), RhoA, RhoGEFs/RhoA (PDZ-RhoGEF + LARG + RhoA), or RhoA/PPARγ. RhoA or RhoGEF/RhoA silencing significantly increase the ABCA1 mRNA (*gray bars*). The simultaneous knockdown of PPARγ with RhoA attenuated the enhancement of ABCA1 mRNA (*black bar*). The *error bars* denote standard deviations of triplicate samples. *, $p < 0.05$.

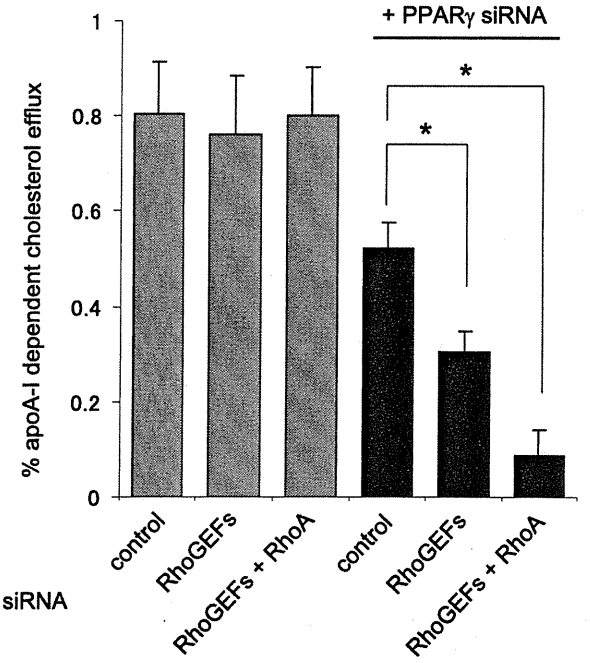

FIGURE 6. **RhoA or RhoGEF/RhoA silencing decreases the cholesterol efflux when PPARγ activity is eliminated.** In RhoGEF- or RhoGEF/RhoA-depleted primary human fibroblasts, cholesterol efflux was not altered because of mRNA compensation of ABCA1 by RhoA inhibition (*gray bars*). When PPARγ was simultaneously knocked down to extinguish the mRNA compensation, RhoGEF or RhoGEF/RhoA silencing causes a significant reduction of efflux activity (*black bars*). The *error bars* denote standard deviations of triplicate samples. *, $p < 0.05$.

motif was found to be required for binding to PDZ-RhoGEF. PDZ-RhoGEF or LARG has been reported to bind transmembrane proteins and receptors including plexin-B1, a receptor for Semaphorin 4D. Semaphorin 4D binding to plexin-B1 stimulates RhoA activation, thus mediating repulsive signals in growth cone guidance of neurons (25). LARG and likely PDZ-RhoGEF associate with the IGF-1 receptor, and IGF-1 activates RhoA and downstream effectors via the LARG/IGF-1 receptor complex and thereby regulates cytoskeletal rearrangements (28). To our knowledge, our results are the first to demonstrate a RhoGEF interaction with an ABC transporter, which is of particular interest in terms of the signaling mechanism by which ABCA1 activates RhoA and which led to the stabilization of ABCA1 protein. In this regard, we found that PDZ-RhoGEF activates RhoA, and this is required for the ability of apoA-I to block ABCA1 protein degradation. Together with the previous observations that the apoA-I stimulation prolongs ABCA1 protein half-life by inhibiting a calpain-mediated degradation pathway (33, 41), our findings indicate that the stabilization of ABCA1 protein mediated by apoA-I depends upon the RhoA activation and the ABCA1/RhoGEF complex.

We previously reported that β1-syntrophin binds ABCA1 and enhances cholesterol efflux by increasing the expression of ABCA1 by protecting it from degradation (8). Syntrophins associate with utrophin, a large scaffolding molecule that links to actin cytoskeleton; thus cell surface ABCA1 is likely stabilized by being anchored to the actin cytoskeleton. We demonstrated here that PDZ-RhoGEF or LARG, which binds to ABCA1, mediates RhoA activation and increases the ABCA1 protein level. These results indicate that ABCA1 is stabilized by multiple mechanisms depending upon its interacting partners. The multiple mechanisms for stabilization could be critically important for proteins like ABCA1, which turns over with a short half-life. Indeed, we demonstrated that the knockdown of PDZ-RhoGEF, LARG (Fig. 6, *black bars*), or β1- or β2-syntrophin (8) in primary human fibroblasts significantly decreased the cholesterol efflux, indicating the importance of these factors for ABCA1 regulation under endogenous expression levels.

Our data that ABCA1 interacts with PDZ-RhoGEF and that apoA-I induces the RhoA activation suggests ABCA1 is not only functioning as a cholesterol transporter but also as a receptor for apolipoproteins to initiate the RhoA signaling (Fig. 7*A*). This model is reasonable because apoA-I can directly bind to ABCA1 (32, 44), and apoA-I stimulates signaling of Cdc42, another Rho GTPase, in normal fibroblasts but not in Tangier

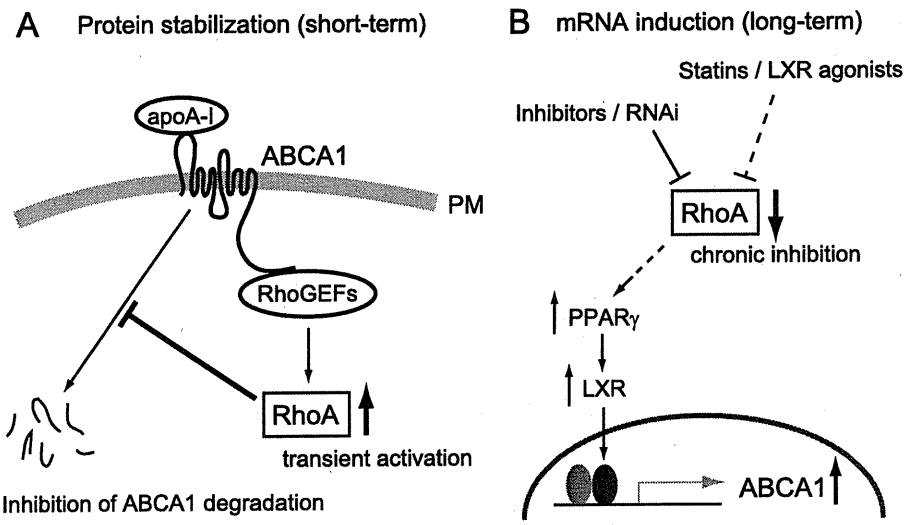

FIGURE 7. **Model for the post-translational (*A*) and transcriptional (*B*) regulation of ABCA1 by RhoA.** *A*, transient activation of RhoA by apoA-I through the binding to the ABCA1/RhoGEF protein complex blocks ABCA1 protein degradation. *B*, chronic inhibition of RhoA induces ABCA1 transcription through PPARγ/LXR pathway.

disease fibroblasts lacking functional ABCA1 (45). Likewise, the cAMP-dependent protein kinase, protein kinase C, and JAK2 kinases are also activated by apoA-I in an ABCA1-dependent manner (46–48). Thus, ABCA1 may act as an apoA-I receptor to transmit signals to the cytoplasm by associating with RhoGEFs, which further modulates the cholesterol efflux process in a feed forward manner by inhibiting the degradation of ABCA1. This mechanism may suggest a model in which the rapid degradation of ABCA1 protein is blocked by the transitory and proximal activation of RhoA during the efflux process when ABCA1 transfers lipid to the bound apoA-I.

This ABCA1 stabilization is likely to be mediated by associating the transporter with the cytoskeletal network because it has reported that the RhoGTPases regulate cytoskeletal dynamics in response to apoA-I binding (45, 49) and agents that disrupt the cytoskeleton (*e.g.* cytochalasin D) also affect cholesterol efflux (50). RhoA was transiently activated by apoA-I with a peak at 5 min and then declined to the basal level (Fig. 4*A*), indicating that RhoA is rapidly deactivated, presumably by the action of RhoGAP proteins (15). Although further work will be needed to validate such a model, these studies may be useful in delineating the potential link between the cytoskeletal dynamics and lipid homeostasis in cells.

Although RhoGEFs stabilize ABCA1 protein in the short term (Fig. 7*A*), the mechanism by which the RhoGEFs and RhoA influence ABCA1 function is complex because our work and previous reports indicate that chronic inhibition of RhoA can also induce ABCA1 expression at the transcriptional level by a mechanism that depends upon PPARγ (Fig. 7*B*). This transcriptional effect needs a longer time compared with the ABCA1 stabilization and is indirect in that it occurs through multiple signaling processes including PPARγ and LXR (42, 43). This long term response may be used by cells to dampen inflammatory signaling pathways because ABCA1 can reduce inflammatory cytokine expression by modifying cell surface lipid raft domains independent of apoA-I (51–54) and LXR agonist treatment of mice causes an anti-inflammatory response that is associated with the inactivation of RhoA (55). Hence, in the pathophysiologic conditions such as the chronic inflammatory environment of the atherosclerotic plaque, RhoA could be inactivated for a longer time frame, leading to the transcriptional induction of ABCA1.

In summary, our results show that PDZ-RhoGEF binds to ABCA1 and positively regulates cholesterol efflux via RhoA activation and stabilization of ABCA1 protein. The binding of apoA-I to the ABCA1/RhoGEF complex stimulates RhoA activation, suggesting that ABCA1 may be playing a receptor function in this RhoA signaling pathway. Given the broad distribution of ABCA1, PDZ-RhoGEF, and RhoA among various tissues, this suggests that a wide range of cells may use this pathway to regulate RhoA signaling and ABCA1 efflux activity.

Acknowledgments—We greatly appreciate the technical assistance of Dr. Sang-Kee Jung, Dr. Kaori Iwasaki, and Dr. Hong-Yan Cui.

REFERENCES

1. Oram, J. F., and Vaughan, A. M. (2006) *Circ. Res.* **99,** 1031–1043
2. Maxfield, F. R., and Tabas, I. (2005) *Nature* **438,** 612–621
3. Miller, N. E., Thelle, D. S., Forde, O. H., and Mjos, O. D. (1977) *Lancet* **1,** 965–968
4. Nissen, S. E., Tsunoda, T., Tuzcu, E. M., Schoenhagen, P., Cooper, C. J., Yasin, M., Eaton, G. M., Lauer, M. A., Sheldon, W. S., Grines, C. L., Halpern, S., Crowe, T., Blankenship, J. C., and Kerensky, R. (2003) *J. Am. Med. Assoc.* **290,** 2292–2300
5. Brooks-Wilson, A., Marcil, M., Clee, S. M., Zhang, L. H., Roomp, K., van Dam, M., Yu, L., Brewer, C., Collins, J. A., Molhuizen, H. O., Loubser, O., Ouelette, B. F., Fichter, K., Ashbourne-Excoffon, K. J., Sensen, C. W., Scherer, S., Mott, S., Denis, M., Martindale, D., Frohlich, J., Morgan, K., Koop, B., Pimstone, S., Kastelein, J. J., Genest, J., Jr., and Hayden, M. R. (1999) *Nat. Genet.* **22,** 336–345
6. Bodzioch, M., Orsó, E., Klucken, J., Langmann, T., Böttcher, A., Diederich, W., Drobnik, W., Barlage, S., Büchler, C., Porsch-Ozcürümez, M., Kaminski, W. E., Hahmann, H. W., Oette, K., Rothe, G., Aslanidis, C., Lackner, K. J., and Schmitz, G. (1999) *Nat. Genet.* **22,** 347–351
7. Rust, S., Rosier, M., Funke, H., Real, J., Amoura, Z., Piette, J. C., Deleuze, J. F., Brewer, H. B., Duverger, N., Denèfle, P., and Assmann, G. (1999) *Nat. Genet.* **22,** 352–355
8. Okuhira, K., Fitzgerald, M. L., Sarracino, D. A., Manning, J. J., Bell, S. A., Goss, J. L., and Freeman, M. W. (2005) *J. Biol. Chem.* **280,** 39653–39664
9. Tamehiro, N., Zhou, S., Okuhira, K., Benita, Y., Brown, C. E., Zhuang, D. Z., Latz, E., Hornemann, T., von Eckardstein, A., Xavier, R. J., Freeman, M. W., and Fitzgerald, M. L. (2008) *Biochemistry* **47,** 6138–6147
10. Munehira, Y., Ohnishi, T., Kawamoto, S., Furuya, A., Shitara, K., Imamura, M., Yokota, T., Takeda, S., Amachi, T., Matsuo, M., Kioka, N., and Ueda, K. (2004) *J. Biol. Chem.* **279,** 15091–15095
11. Hozoji, M., Munehira, Y., Ikeda, Y., Makishima, M., Matsuo, M., Kioka, N., and Ueda, K. (2008) *J. Biol. Chem.* **283,** 30057–30063
12. Buechler, C., Bared, S. M., Aslanidis, C., Ritter, M., Drobnik, W., and

Schmitz, G. (2002) *J. Biol. Chem.* **277,** 41307–41310
13. Bared, S. M., Buechler, C., Boettcher, A., Dayoub, R., Sigruener, A., Grandl, M., Rudolph, C., Dada, A., and Schmitz, G. (2004) *Mol. Biol. Cell* **15,** 5399–5407
14. Schmidt, A., and Hall, A. (2002) *Genes Dev.* **16,** 1587–1609
15. Siderovski, D. P., and Willard, F. S. (2005) *Int. J. Biol. Sci.* **1,** 51–66
16. Hart, M. J., Jiang, X., Kozasa, T., Roscoe, W., Singer, W. D., Gilman, A. G., Sternweis, P. C., and Bollag, G. (1998) *Science* **280,** 2112–2114
17. Kozasa, T., Jiang, X., Hart, M. J., Sternweis, P. M., Singer, W. D., Gilman, A. G., Bollag, G., and Sternweis, P. C. (1998) *Science* **280,** 2109–2111
18. Fukuhara, S., Murga, C., Zohar, M., Igishi, T., and Gutkind, J. S. (1999) *J. Biol. Chem.* **274,** 5868–5879
19. Rümenapp, U., Blomquist, A., Schwörer, G., Schablowski, H., Psoma, A., and Jakobs, K. H. (1999) *FEBS Lett.* **459,** 313–318
20. Fukuhara, S., Chikumi, H., and Gutkind, J. S. (2000) *FEBS Lett.* **485,** 183–188
21. Togashi, H., Nagata, K., Takagishi, M., Saitoh, N., and Inagaki, M. (2000) *J. Biol. Chem.* **275,** 29570–29578
22. Reuther, G. W., Lambert, Q. T., Booden, M. A., Wennerberg, K., Becknell, B., Marcucci, G., Sondek, J., Caligiuri, M. A., and Der, C. J. (2001) *J. Biol. Chem.* **276,** 27145–27151
23. Aurandt, J., Vikis, H. G., Gutkind, J. S., Ahn, N., and Guan, K. L. (2002) *Proc. Natl. Acad. Sci. U.S.A.* **99,** 12085–12090
24. Perrot, V., Vazquez-Prado, J., and Gutkind, J. S. (2002) *J. Biol. Chem.* **277,** 43115–43120
25. Swiercz, J. M., Kuner, R., Behrens, J., and Offermanns, S. (2002) *Neuron* **35,** 51–63
26. Hirotani, M., Ohoka, Y., Yamamoto, T., Nirasawa, H., Furuyama, T., Kogo, M., Matsuya, T., and Inagaki, S. (2002) *Biochem. Biophys. Res. Commun.* **297,** 32–37
27. Driessens, M. H., Olivo, C., Nagata, K., Inagaki, M., and Collard, J. G. (2002) *FEBS Lett.* **529,** 168–172
28. Taya, S., Inagaki, N., Sengiku, H., Makino, H., Iwamatsu, A., Urakawa, I., Nagao, K., Kataoka, S., and Kaibuchi, K. (2001) *J. Cell Biol.* **155,** 809–820
29. Yamada, T., Ohoka, Y., Kogo, M., and Inagaki, S. (2005) *J. Biol. Chem.* **280,** 19358–19363
30. Bourguignon, L. Y., Gilad, E., Brightman, A., Diedrich, F., and Singleton, P. (2006) *J. Biol. Chem.* **281,** 14026–14040
31. Fitzgerald, M. L., Okuhira, K., Short, G. F., 3rd, Manning, J. J., Bell, S. A., and Freeman, M. W. (2004) *J. Biol. Chem.* **279,** 48477–48485
32. Fitzgerald, M. L., Morris, A. L., Rhee, J. S., Andersson, L. P., Mendez, A. J., and Freeman, M. W. (2002) *J. Biol. Chem.* **277,** 33178–33187
33. Arakawa, R., and Yokoyama, S. (2002) *J. Biol. Chem.* **277,** 22426–22429
34. Fitzgerald, M. L., Mendez, A. J., Moore, K. J., Andersson, L. P., Panjeton, H. A., and Freeman, M. W. (2001) *J. Biol. Chem.* **276,** 15137–15145
35. Abe-Dohmae, S., Ikeda, Y., Matsuo, M., Hayashi, M., Okuhira, K., Ueda, K., and Yokoyama, S. (2004) *J. Biol. Chem.* **279,** 604–611
36. Kim, W. S., Fitzgerald, M. L., Kang, K., Okuhira, K., Bell, S. A., Manning, J. J., Koehn, S. L., Lu, N., Moore, K. J., and Freeman, M. W. (2005) *J. Biol. Chem.* **280,** 3989–3995
37. Jehle, A. W., Gardai, S. J., Li, S., Linsel-Nitschke, P., Morimoto, K., Janssen, W. J., Vandivier, R. W., Wang, N., Greenberg, S., Dale, B. M., Qin, C., Henson, P. M., and Tall, A. R. (2006) *J. Cell Biol.* **174,** 547–556
38. Iwamoto, N., Abe-Dohmae, S., Sato, R., and Yokoyama, S. (2006) *J. Lipid Res.* **47,** 1915–1927
39. Rogler, G., Trümbach, B., Klima, B., Lackner, K. J., and Schmitz, G. (1995) *Arterioscler. Thromb. Vasc. Biol.* **15,** 683–690
40. Remaley, A. T., Schumacher, U. K., Stonik, J. A., Farsi, B. D., Nazih, H., and Brewer, H. B., Jr. (1997) *Arterioscler. Thromb. Vasc. Biol.* **17,** 1813–1821
41. Wang, N., Chen, W., Linsel-Nitschke, P., Martinez, L. O., Agerholm-Larsen, B., Silver, D. L., and Tall, A. R. (2003) *J. Clin. Invest.* **111,** 99–107
42. Argmann, C. A., Edwards, J. Y., Sawyez, C. G., O'Neil, C. H., Hegele, R. A., Pickering, J. G., and Huff, M. W. (2005) *J. Biol. Chem.* **280,** 22212–22221
43. Yano, M., Matsumura, T., Senokuchi, T., Ishii, N., Murata, Y., Taketa, K., Motoshima, H., Taguchi, T., Sonoda, K., Kukidome, D., Takuwa, Y., Kawada, T., Brownlee, M., Nishikawa, T., and Araki, E. (2007) *Circ. Res.* **100,** 1442–1451
44. Wang, N., Silver, D. L., Thiele, C., and Tall, A. R. (2001) *J. Biol. Chem.* **276,** 23742–23747
45. Nofer, J. R., Remaley, A. T., Feuerborn, R., Wolinnska, I., Engel, T., von Eckardstein, A., and Assmann, G. (2006) *J. Lipid Res.* **47,** 794–803
46. Yamauchi, Y., Hayashi, M., Abe-Dohmae, S., and Yokoyama, S. (2003) *J. Biol. Chem.* **278,** 47890–47897
47. Tang, C., Vaughan, A. M., and Oram, J. F. (2004) *J. Biol. Chem.* **279,** 7622–7628
48. Haidar, B., Denis, M., Marcil, M., Krimbou, L., and Genest, J., Jr. (2004) *J. Biol. Chem.* **279,** 9963–9969
49. Nofer, J. R., Feuerborn, R., Levkau, B., Sokoll, A., Seedorf, U., and Assmann, G. (2003) *J. Biol. Chem.* **278,** 53055–53062
50. Walter, M., Forsyth, N. R., Wright, W. E., Shay, J. W., and Roth, M. G. (2004) *J. Biol. Chem.* **279,** 20866–20873
51. Yvan-Charvet, L., Ranalletta, M., Wang, N., Han, S., Terasaka, N., Li, R., Welch, C., and Tall, A. R. (2007) *J. Clin. Invest.* **117,** 3900–3908
52. Francone, O. L., Royer, L., Boucher, G., Haghpassand, M., Freeman, A., Brees, D., and Aiello, R. J. (2005) *Arterioscler. Thromb. Vasc. Biol.* **25,** 1198–1205
53. Koseki, M., Hirano, K., Masuda, D., Ikegami, C., Tanaka, M., Ota, A., Sandoval, J. C., Nakagawa-Toyama, Y., Sato, S. B., Kobayashi, T., Shimada, Y., Ohno-Iwashita, Y., Matsuura, F., Shimomura, I., and Yamashita, S. (2007) *J. Lipid Res.* **48,** 299–306
54. Zhu, X., Lee, J. Y., Timmins, J. M., Brown, J. M., Boudyguina, E., Mulya, A., Gebre, A. K., Willingham, M. C., Hiltbold, E. M., Mishra, N., Maeda, N., and Parks, J. S. (2008) *J. Biol. Chem.* **283,** 22930–22941
55. Smoak, K., Madenspacher, J., Jeyaseelan, S., Williams, B., Dixon, D., Poch, K. R., Nick, J. A., Worthen, G. S., and Fessler, M. B. (2008) *J. Immunol.* **180,** 3305–3312

Bioorganic & Medicinal Chemistry Letters 22 (2012) 1793–1796

Contents lists available at SciVerse ScienceDirect

Bioorganic & Medicinal Chemistry Letters

journal homepage: www.elsevier.com/locate/bmcl

Design and synthesis of estrogen receptor degradation inducer based on a protein knockdown strategy

Yosuke Demizu [a], Keiichiro Okuhira [b], Hiromi Motoi [a], Akiko Ohno [a], Takuji Shoda [a], Kiyoshi Fukuhara [a], Haruhiro Okuda [a], Mikihiko Naito [b,*], Masaaki Kurihara [a,*]

[a] Division of Organic Chemistry, National Institute of Health Sciences, 1-18-1, Kamiyoga, Setagaya, Tokyo 158-8501, Japan
[b] Division of Biochemistry and Molecular Biology, National Institute of Health Sciences, 1-18-1, Kamiyoga, Setagaya, Tokyo 158-8501, Japan

ARTICLE INFO

Article history:
Received 1 November 2011
Revised 18 November 2011
Accepted 21 November 2011
Available online 28 November 2011

Keywords:
Estrogen receptor
Protein knockdown
Tamoxifen
Ubiquitin-proteasome system

ABSTRACT

We designed and synthesized estrogen receptor (ER) degradation inducers 5, 6, and 7, which crosslink the ER and the cellular inhibitor of apoptosis protein 1 (cIAP1). Compounds **5**, **6**, and **7** induced cIAP1-mediated ubiquitylation of ERα resulting in its proteasomal degradation.

Breast cancer is the most common form of cancer in women, and its incidence is increasing year by year. Estrogen receptors (ERs) are often overexpressed in the tissues of breast cancer patients, which promotes the estrogen-dependent proliferation of cancer cells.[1–3] Therefore, ER antagonistic drugs, such as tamoxifen, a non-steroidal selective estrogen receptor modulator, are effective at treating breast cancer.[4,5] Tamoxifen is metabolized by CYP2D6 and CYP3A4 into 4-hydroxytamoxifen, which has 30–100 times more affinity for the estrogen receptor than tamoxifen itself.[6] Tamoxifen is the most frequently prescribed drug for the treatment of all stages of breast cancer,[7] and it is also used to prevent the disease in women who are at high risk of developing breast cancer.[8] However, tamoxifen has agonistic effects on ER in uterus cancer cells and increases the risk of endometrial cancer.[9,10] Furthermore, tamoxifen activates the protein kinase B (Akt) signaling pathway by binding to a particular ER variant, resulting in the inhibition of apoptosis in cancer cells.[11,12]

Recently, we reported a protein knockdown strategy for inducing the degradation of a target protein using the ubiquitin-proteasome system (UPS).[13–18] To degrade proteins of interest, we developed SNIPER (*S*pecific and *N*on-genetic *I*AP-dependent *P*rotein *E*rasers), hybrid molecules composed of bestatin (BS), an inhibitor of the cellular apoptosis protein 1 (cIAP1), and a ligand for the target protein.[13–15] These molecules cross-link cIAP1 and the target protein to induce ubiquitylation and subsequent proteasomal degradation of the target protein.

In this study, we applied this methodology to the selective degradation of ERα in breast cancer cells. We designed SNIPER(ER) hybrid molecules **5**, **6**, and **7**, which induce the selective poly-ubiquitylation of the ER to cause proteasomal degradation. Molecules **5**, **6**, and **7** contain two biologically active scaffolds: one is a tamoxifen derivative, which is used to bind to the ER, and the other is a BS moiety, which binds to cIAP1 to induce the ubiquitylation and subsequent proteasomal degradation of the target protein (Fig. 1). Molecules with different length linkers **5**, **6**, and **7** were designed based on the X-ray structure (PDB ID: 3ERT) of the complex formed between 4-hydroxytamoxifen and ERα,[19] and BS was ligated to the dimethylamino moiety of 4-hydroxytamoxifen (red circle in Fig. 2a) via an alkyl linker (Fig. 2b).

The ligated molecules **5**, **6**, and **7** were synthesized as follows (Scheme 1). First, (*E*/*Z*)-endoxifen (**1**)[20,21] was condensed with several acids to afford amides **2**, **3**, and **4**. After deprotection of one of the *N*-Boc protecting groups of **2**, **3**, and **4**, the generated amines were reacted with *N*-Boc bestatin,[11] and the subsequent deprotection of another of the molecules' *N*-Boc protecting groups gave ligated compounds **5**, **6**, and **7**, respectively.[22]

Then, we evaluated the effects of compounds **5**, **6**, and **7** on ERα protein degradation in MCF-7 breast cancer cells by examining the treatment dose (Fig. 3).[23] The protein expression of ERα was increased by treatment with (*E*/*Z*)-endoxifen (lane 3), which was consistent with the findings of a previous report demonstrating that (*E*/*Z*)-endoxifen induced the accumulation of ERα protein in

* Corresponding authors. Tel.: +81 3 3700 1141; fax: +81 3 3707 6950.
E-mail addresses: miki-naito@nihs.go.jp (M. Naito), masaaki@nihs.go.jp (M. Kurihara).

0960-894X/$ - see front matter © 2012 Published by Elsevier Ltd.
doi:10.1016/j.bmcl.2011.11.086

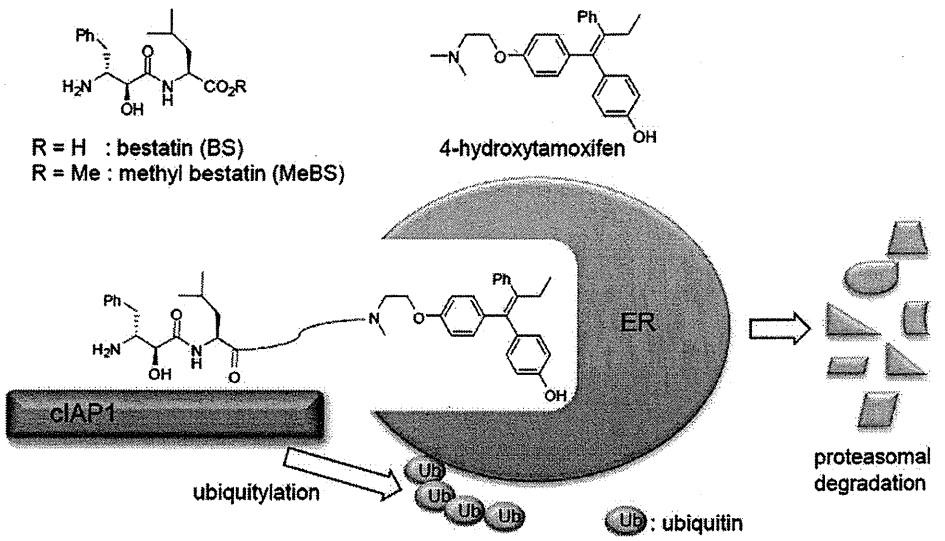

Figure 1. Estrogen receptor degradation strategy using a ligated hybrid molecule.

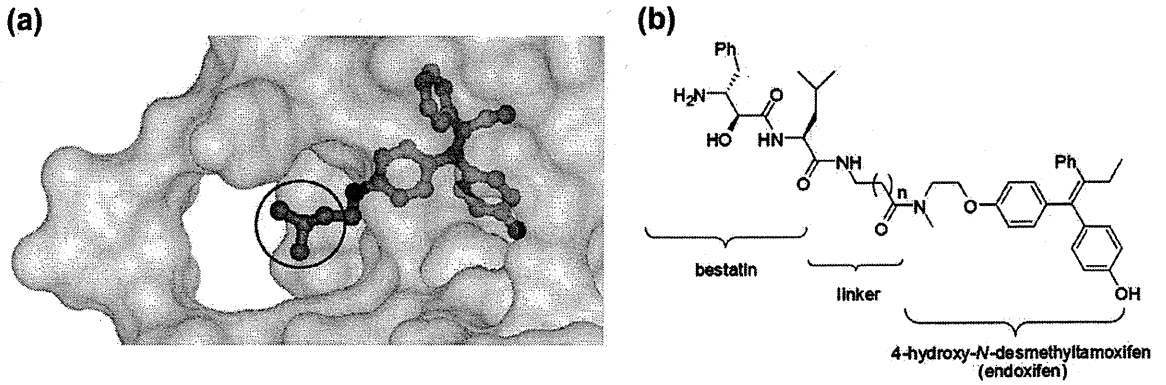

Figure 2. (a) X-ray structure of the complex formed between 4-hydroxytamoxifen and ERα(3ERT). (b) Design of the SNIPER(ER) ER degradation inducer.

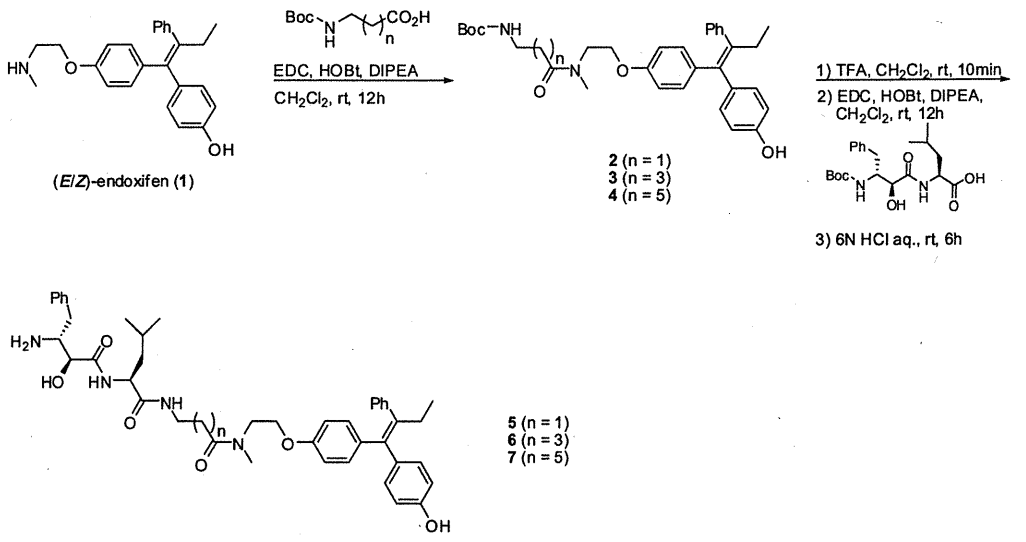

Scheme 1. Synthesis of ligated compounds **5**, **6**, and **7**.

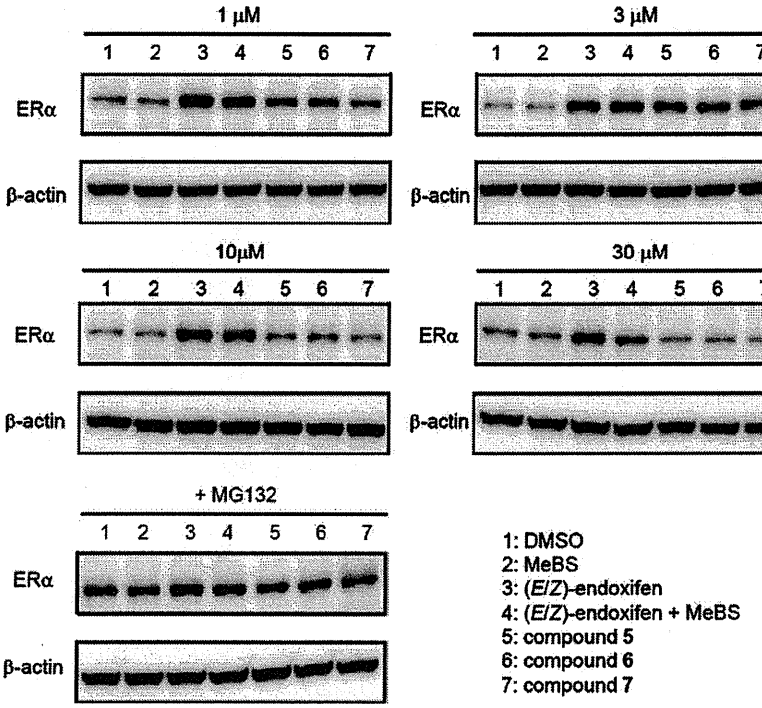

Figure 3. Dose-dependent ERα degradation responses induced by compounds **5**, **6**, and **7** and the effects of a protease inhibitor on these responses.

MCF-7 cells.[24] Compared with (*E*/*Z*)-endoxifen (lane 3), a reduced level of ERα was observed in the cells treated with 10 or 30 μM of compound **5**, **6**, or **7** (lanes 5, 6, and 7, respectively), and no apparent differences in the activities of them were observed during the 6 h study period. On the other hand, the ERα level was not altered by the combined use of (*E*/*Z*)-endoxifen and methyl bestatin (MeBS)[25] (lane 4). These results suggest that (*E*/*Z*)-endoxifen conjugated with BS as a single molecule (at a concentration of greater than 10 μM) is required for the efficient degradation of the ERα protein. Furthermore, the suppressive effects of compounds **5**, **6**, and **7** on ERα were blocked by the addition of a proteasome inhibitor, MG132, indicating that compounds **5**, **6**, and **7** induced the proteasomal degradation of ERα.

In summary, we used a protein knockdown method for the selective degradation of ERα and synthesized ERα degradation inducers **5**, **6**, and **7**, which form crosslinks between ERα and cIAP1. Compounds **5**, **6**, and **7** were able to induce cIAP1-mediated ubiquitylation and hence induce the proteasomal degradation of ERα. These molecules are novel candidates for therapeutic agents against breast cancer, and further derivatization of these molecules is currently underway.

Acknowledgments

This study was supported, in part, by Grants-in-Aid for Scientific Research (C) (M.K.: 22590114) and Challenging Exploratory Research (M.N.: 23659048) from the Japan Society for the Promotion of Science, a research grant from the Astellas Foundation for Research on Metabolic Disorders (M.N.), and a grant from the Terumo Life Science Foundation (M.N.).

References and notes

1. Holst, F.; Stahl, P. R.; Ruiz, C.; Hellwinkel, O.; Jehan, Z.; Wendland, M.; Lebeau, A.; Terracciano, L.; Al-Kuraya, K.; Jänicke, F.; Sauter, G.; Simon, R. *Nat. Genet.* **2007**, *39*, 655.
2. Doisneau-Sixou, S. F.; Cergio, C. M.; Carroll, J. S.; Hui, R.; Musgrove, E. A.; Sutherland, R. L. *Endocrine-Related Cancer* **2003**, *10*, 179.
3. Foster, J. S.; Henley, D. C.; Bukovsky, A.; Seth, P.; Wimalasena, J. *Mol. Cell. Biol.* **2001**, *21*, 794.
4. Deroo, B. J.; Korach, K. S. *J. Clin. Invest.* **2006**, *116*, 561.
5. Early Breast Cancer Trialists' Collaborative Group *Lancet* **1998**, *351*, 1451.
6. Desta, Z.; Ward, B. A.; Soukhova, N. V.; Flockhart, D. A. *J. Pharmacol. Exp. Ther.* **2004**, *310*, 1062.
7. Early Breast Cancer Trialists' Collaborative Group *Lancet* **1992**, *339*, 71.
8. Fisher, B.; Costantino, J. P.; Wickerham, D. L.; Redmond, C. K.; Kavanah, M.; Cronin, W. M.; Vogel, V.; Robidoux, A.; Dimitrov, N.; Atkins, J.; Daly, M.; Wieand, S.; Tan-Chiu, E.; Ford, L.; Wolmark, N. *J. Natl. Cancer Inst. (Bethesda)* **1998**, *90*, 1371.
9. Bernstein, L.; Deapen, D.; Cerhan, J. R.; Schwartz, S. M.; Liff, J.; McGann-Maloney, E.; Perlman, J. A.; Ford, L. *J. Natl. Cancer Inst.* **1999**, *91*, 1654.
10. Shang, Y.; Brown, M. *Science* **2002**, *295*, 2465.
11. Arpino, G.; Wiechmann, L.; Osborne, C. K.; Schiff, R. *Endocr. Rev.* **2008**, *29*, 217.
12. Lin, S.-L.; Yan, L.-Y.; Zhang, X.-T.; Yuan, J.; Li, M.; Qiao, J.; Wang, Z.-Y.; Sheng, J.; Sun, Q.-Y. *PLoS One* **2010**, *5*, e9013.
13. Itoh, Y.; Ishikawa, M.; Naito, M.; Hashimoto, Y. *J. Am. Chem. Soc.* **2010**, *132*, 5820.
14. Itoh, Y.; Ishikawa, M.; Kitaguchi, R.; Sato, S.; Naito, M.; Hashimoto, Y. *Bioorg. Med. Chem.* **2011**, *19*, 3229.
15. Okuhira, K.; Ohoka, N.; Sai, K.; Nishimaki-Mogami, T.; Itoh, Y.; Ishikawa, M.; Hashimoto, Y.; Naito, M. *FEBS Lett.* **2011**, *585*, 1147.
16. Sekine, K.; Takubo, K.; Kikuchi, R.; Nishimoto, M.; Kitagawa, M.; Abe, F.; Nishikawa, K.; Tsuruo, T.; Naito, M. *J. Biol. Chem.* **2008**, *283*, 8961.
17. Kim, S.; Ohoka, N.; Okuhira, K.; Sai, K.; Nishimaki-Mogami, T.; Naito, M. *Cancer Sci.* **2010**, *101*, 2425.
18. Sato, S.; Aoyama, H.; Miyachi, H.; Naito, M.; Hashimoto, Y. *Bioorg. Med. Chem. Lett.* **2008**, *18*, 3354.
19. Shiau, A. K.; Barstad, D.; Loria, P. M.; Cheng, L.; Kushner, P. J.; Agard, D. A.; Greene, G. L. *Cell* **1998**, *95*, 927.
20. We used (*E*/*Z*)-endoxifen because (*E*)- and (*Z*)-4-hydroxytamoxifen derivatives are isomerized in vivo: Crewe, H. K.; Notley, L. M.; Wunsch, R. M.; Lennard, M. S.; Gillam, E. M. *Drug Metab. Dispos.* **2002**, *30*, 869.
21. Preparation of (*E*/*Z*)-endoxifen: Fauq, A. H.; Maharvi, G. M.; Sinha, D. *Bioorg. Med. Chem. Lett.* **2010**, *20*, 3036.
22. *Spectroscopic data for compound* **7**: White solid; ^{1}H NMR (400 MHz, CD_3OD) δ 6.91–7.35 (m, 13H), 6.40–6.76 (m, 5H), 3.98–4.34 (m, 4H), 3.66–3.83 (m, 3H), 2.91–3.18 (m, 7H), 2.30–2.47 (m, 4H), 1.28–1.84 (m, 11H), 0.89–0.99 (m, 9H); ^{13}C NMR (100 MHz, CD_3OD) 175.2, 173.1, 172.0, 142.9, 141.0, 138.5, 136.7, 136.4, 135.5, 135.1, 131.8, 130.4, 129.7, 129.3, 128.9, 128.6, 128.1, 127.7, 127.4, 125.8, 114.7, 113.9, 113.1, 68.6, 65.4, 55.1, 52.4, 40.9, 39.2, 35.3, 33.0, 32.5, 29.7, 29.2, 28.9, 26.4, 25.3, 24.9, 22.1, 21.2, 12.8; [HR-ESI(+)]: *m*/*z* calcd for $C_{48}H_{63}N_4O_6$ $[M+H]^+$ 791.4748: found 791.4852.

23. MCF-7 cells were treated with the test compounds at the indicated concentrations in the presence or absence of 10 μM of MG132 for 6 h, and then the cells were collected and extracted with lysis buffer (1% SDS, 0.1 M Tris–HCl (pH 7.0), 10% glycerol) and boiled for 10 min. Protein concentrations were determined by the BCA method, and equal amounts of protein lysate were separated by SDS–PAGE, transferred to a PVDF membrane, and Western blotted using the following antibodies: anti-human ERα mouse monoclonal antibody (Santa Cruz), anti-β-actin mouse monoclonal antibody (SIGMA), and anti-human cIAP1 goat polyclonal antibody (R&D systems).
24. Laïos, I.; Journe, F.; Laurent, G.; Nonclercq, D.; Toillon, R. A.; Seo, H. S.; Leclercq, G. *J. Steroid Biochem. Mol. Biol.* **2003**, *87*, 207.
25. MeBS interacts with the BIR3 domain of cIAP1 and induces the auto-ubiquitylation of cIAP-1, resulting in the proteasomal degradation of cIAP1: See Ref. 16.

FEBS Letters 585 (2011) 1147–1152

FEBS Letters

journal homepage: www.FEBSLetters.org

Specific degradation of CRABP-II via cIAP1-mediated ubiquitylation induced by hybrid molecules that crosslink cIAP1 and the target protein

Keiichiro Okuhira [a], Nobumichi Ohoka [a], Kimie Sai [a], Tomoko Nishimaki-Mogami [a], Yukihiro Itoh [b], Minoru Ishikawa [b], Yuichi Hashimoto [b], Mikihiko Naito [a,*]

[a] Division of Biochemistry and Molecular Biology, National Institute of Health Sciences, Japan
[b] Institute of Molecular and Cellular Biosciences, The University of Tokyo, Japan

ARTICLE INFO

Article history:
Received 12 January 2011
Revised 7 March 2011
Accepted 8 March 2011
Available online 15 March 2011

Edited by Noboru Mizushima

Keywords:
Cellular inhibitor of apoptosis protein 1
Cellular retinoic acid binding protein-II
Protein knockdown
Ubiquitin
Proteasome

ABSTRACT

Manipulation of protein stability with small molecules is a challenge in the field of drug discovery. Here we show that cellular retinoic acid binding protein-II (CRABP-II) can be specifically degraded by a novel compound, SNIPER-4, consisting of (−)-*N*-[(2*S*,3*R*)-3-amino-2-hydroxy-4-phenylbutyryl]-L-leucine methyl ester and all-trans retinoic acid that are ligands for cellular inhibitor of apoptosis protein 1 (cIAP1) and CRABP-II, respectively. Mechanistic analysis revealed that SNIPER-4 induces cIAP1-mediated ubiquitylation of CRABP-II, resulting in the proteasomal degradation. The protein knockdown strategy employing the structure of SNIPER-4 could be applicable to other target proteins.

1. Introduction

The ubiquitin–proteasome system (UPS) plays a crucial role in selective degradation of proteins, which is involved in the regulation of cell cycle, proliferation, differentiation and cell death [1–3]. In the UPS, the target protein is poly-ubiquitylated by the sequential action of ubiquitin-activating enzyme (E1), ubiquitin-conjugating enzyme (E2) and ubiquitin-ligase (E3), where E3 determines the specificity for the target protein in many cases. The poly-ubiquitylated proteins are degraded by proteasome. Inappropriate regulation of the UPS results in an accumulation or depletion of certain proteins, which results in a variety of diseases such as cancer, cachexia, neurodegenerative disorders and malformation [4–8]. To reduce a pathogenic protein in cells, it is useful to take advantage of the UPS since it is a highly specific system to target a certain protein for degradation, and the degradation occurs very quickly. However, few studies have been reported so far on the specific degradation of target proteins utilizing the UPS [9].

We previously reported that a class of small molecules, represented by (−)-*N*-[(2*S*,3*R*)-3-amino-2-hydroxy-4-phenyl-butyryl]-L-leucine methyl ester (MeBS), destabilize cellular inhibitor of apoptosis protein 1 (cIAP1), a ubiquitin-ligase (E3) belonging to IAP (inhibitor of apoptosis protein) family [10–12], and sensitize cancer cells to apoptosis induced by anti-cancer drugs and death receptor ligation [13–16]. MeBS directly interacts with cIAP1 at its BIR3 domain and induces auto-ubiquitylation of cIAP1 depending on its RING domain, resulting in the proteasomal degradation of cIAP1. Structure–activity relationship study indicated that analogs with a carboxyl-ester reduce the amount of cIAP1 even though the methyl group is substituted to other residues, and other modifications of MeBS seriously affected the activity [13]. Based on these observations, we hypothesized that the methyl group can be substituted to a ligand for a target protein without ablating the ubiquitin ligase activity of cIAP1. The hybrid molecule consisting of MeBS and the ligand would be able to cross-link cIAP1 and the target protein, to induce ubiquitylation and proteasomal degradation of the target protein. As a proof-of-concept study, we designed and synthesized a series of hybrid compounds consisting of MeBS and all-trans retinoic acid (ATRA), and found that they

Abbreviations: cIAP1, cellular inhibitor of apoptosis protein 1; MeBS, (−)-*N*-[(2*S*,3*R*)-3-amino-2-hydroxy-4-phenyl-butyryl]-L-leucine methyl ester; ATRA, all-trans retinoic acid; CRABP, cellular retinoic acid binding protein

* Corresponding author. Address: Division of Biochemistry and Molecular Biology, National Institute of Health Sciences, 1-18-1, Kamiyoga, Setagaya-ku, Tokyo 158-8501, Japan. Fax: +81 3 3707 6950.
E-mail address: miki-naito@nihs.go.jp (M. Naito).

0014-5793/$36.00 © 2011 Federation of European Biochemical Societies. Published by Elsevier B.V. All rights reserved.
doi:10.1016/j.febslet.2011.03.019

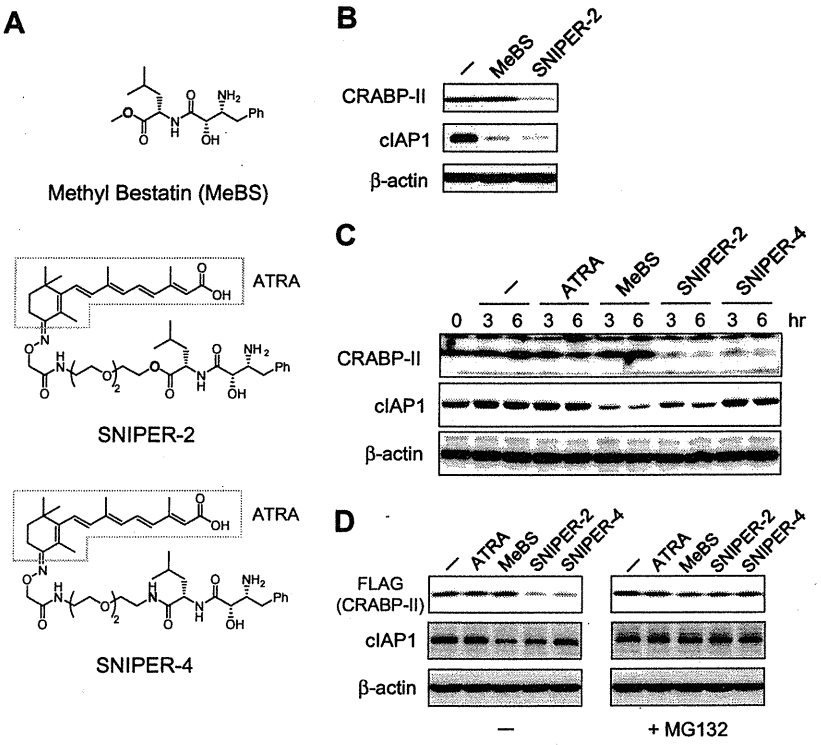

Fig. 1. Structure and protein knockdown activity of SNIPERs. (A) Structures of MeBS (top), SNIPER-2 (middle) and SNIPER-4 (bottom). (B) Reduction of endogenous CRABP-II and cIAP1 by SNIPER-2. (C) SNIPER-4 reduces endogenous CRABP-II but not cIAP1. (D) Inhibition of the SNIPER-mediated protein knockdown by a proteasome inhibitor, MG132. Human primary fibroblasts (B), HT1080 (C) or HT1080 cells expressing FLAG-CRABP-II (D) were incubated with 10 μM of indicated compounds for 6 h. Cells were pretreated with 10 μM of MG132 for 30 min in (D). Shown are immunoblots of cell lysates stained with indicated antibodies.

induce the proteasomal degradation of CRABP-II, an ATRA-binding protein [17]. Thus, selective degradation of target protein (protein knockdown) can be attained by the hybrid molecules that cross-link the target protein and cIAP1.

The hybrid molecule we have developed previously [17], which we named SNIPER (Specific and Non-genetic IAP-dependent Protein ERaser)-2 in this study, however, has two major downsides that would be unfavorable for protein knockdown: (1) SNIPER-2 causes a simultaneous degradation of cIAP1 with the target protein CRABP-II, which may make the protein knockdown unsustainable, and (2) SNIPER-2 contains an ester-bond which is vulnerable to hydrolysis. To overcome these issues, we here developed SNIPER-4, in which the ester-bond is substituted to amide-bond, and found that the SNIPER-4 induces specific and sustained degradation of CRABP-II without inducing cIAP1 degradation. We also investigated biochemical mechanisms by which SNIPERs target CRABP-II for degradation, and demonstrate that SNIPERs induce the ubiquitylation of CRABP-II, which is mediated by cIAP1 but not by XIAP.

2. Materials and methods

2.1. Reagents and plasmids

MeBS was kindly provided by Nippon Kayaku Co. Ltd. (Tokyo, Japan). SNIPER-2 was synthesized as described previously [17]. The synthesis and structural analysis of SNIPER-4 would be reported elsewhere (Itoh et al., manuscript in preparation). cDNA encoding human CRABP-II were amplified by PCR from JHH-5 cDNA library and cloned into a p3xFLAG-CMV-10 expression vector (SIGMA). The correct DNA sequence was confirmed. The following reagents were purchased from indicated supplier: M2 anti-FLAG mouse monoclonal antibody, M2 anti-FLAG agarose-conjugated antibody, mouse anti-β-actin antibody (SIGMA); Fugene HD, anti-HA rat monoclonal antibody (Roche); CRABP-II antibody (Abcam); anti-human cIAP1 goat polyclonal antibody (R&D systems); anti-human XIAP mouse monoclonal antibody (MBL); Lipofectamine RNAi MAX transfection reagent, Stealth Select RNAi (Invitrogen). The target sequences for cIAP1 and XIAP RNAi were as follows: cIAP1-#1 (5′-TCTAGAGCAGTTGAAGACATCTCTT-3′); cIAP1-#2 (5′-GGAAATGCTGCGGCCAACATCTTCA-3′); XIAP-#1 (5′-ACACTGGCACGAGCAGGGTTTCTTT-3′); XIAP-#2 (5′-CCAGAATGGTCAGTACAAAGTTGAA-3′).

2.2. Cell culture, transfection and treatment with compounds

Human fibrosarcoma HT1080 were maintained in RPMI 1640 medium containing 10% fetal bovine serum and 100 μg/ml of kanamycin. Transient transfections were carried out using Fugene HD according to the manufacturer's instructions. siRNA transfections were carried out by reverse transfection method with Lipofectamine RNAi MAX according to the manufacturer's instructions. In brief, 60 pmol siRNA and 3 μl of Lipofectamine RNAi MAX were incubated in 200 μl Opti-MEM medium for 20 min at room temperature in 12-well plates, and then 1 ml of cell suspension (1.5×10^5 cells) was added to the siRNA–RNAi MAX complex. HT1080 cells constitutively expressing FLAG-CRABP-II were generated and maintained in RPMI 1640 medium containing 10% fetal bovine serum and 100 μg/ml of kanamycin and 500 μg/ml of Geneticin (G418). The cells were treated with 10 μM SNIPERs or vehicle (DMSO) for 6 h unless otherwise indicated, and lysed in